

NASA Technical Memorandum 89026

THERMAL ANALYSIS OF RADIOMETER CONTAINERS FOR THE 122 METER HOOP COLUMN ANTENNA (HCA) CONCEPT

(NASA-TM-89026) THERMAL ANALYSIS OF
RADIOMETER CONTAINERS FOR THE 122m HOOP
COLUMN ANTENNA CONCEPT (NASA) 54 p CSCL 20D

N87-11966

Unclas
G3/34 44873

L. A. DILLON-TOWNES

SEPTEMBER 1986



National Aeronautics and
Space Administration

Langley Research Center
Hampton, Virginia 23665

TABLE OF CONTENTS

	PAGE
SUMMARY	1
INTRODUCTION	1
RADIOMETER CONTAINER CONCEPT	2
THERMAL ANALYSIS	3
- Orbit Definition	4
- Geometric Definitions	4
- Heat Flux Model	5
- Surface Temperature	5
RESULTS.....	6
- Top Radiometer Container	7
- Bottom Radiometer Container	7
CONCLUSION	7
RECOMMENDATIONS	7
REFERENCES AND BIBLIOGRAPHY.....	9
APPENDICES	36
- Appendix A: TRASYS Radiation Model	38
MITAS Thermal Model	42
- Appendix B: "Average" Surface Temperatures	47

SUMMARY

The thermal analysis presented in this paper is a first step in the design of thermal containers to house the electronics for the 122 m Hoop Column Antenna Radiometer concept. The analysis accounts for geometric peculiarities, orbital parameters, and thermal considerations. The analysis used a computer aided graphics package called ANVIL 4000 (ref. 9) to develop the geometric configuration of the radiometer containers. Also, two thermal models were developed to obtain the container surface temperatures. The first model was developed using a computer software system called TRASYS (ref. 10) which solves radiation relationships for thermal problems. Incident and absorbed heat rate data from environmental radiant heat sources to nodes are provided, in addition to radiation interchange data between nodes. The TRASYS model which consisted of 28 nodes provided orbital heat inputs to the radiometer containers which were used by the second thermal model.

The second model was developed using a finite difference thermal analysis computer code called MITAS II (ref. 11). The MITAS II model which consisted of 28 nodes and 94 conductors, accepted the environmental heat loads generated by the TRASYS model and calculated the surface temperatures of each container for selected emittance (ϵ) and solar absorptance (α_s ; ref. 12).

The results of the thermal analysis provide relationships between α_s/ϵ ratios and the "average" surface temperature for each orbiting radiometer container. Using these graphic relationships one can specify the thermal surface properties of the containers in terms of absorptance and emittance or, an average surface temperature for each container can be determined if surface material is known. Finally, the thermal models developed for this analysis can be used to define the total thermal control system required for each container of the radiometer instrument. This paper makes an initial attempt to look at the surface temperatures of the containers for selected solar absorptance and emittance ratios. The models can also be used to determine the inside wall temperatures of the containers, the quantity of heat to be removed by an active thermal system, and ultimately to obtain a heat balance for the containers so that the critical electronic components can be thermally stabilized. Furthermore, the thermal models could be used for comparison when actual instrument testing is conducted.

INTRODUCTION

NASA Langley Research Center has been interested in demonstrating the technology of obtaining geophysical parameters such as soil moisture, sea surface temperature, wind speed, and salinity for several years. Several aircraft instruments have been developed to obtain these data. A recently developed instrument, the "Pushbroom Microwave Radiometer" (ref. 1) serves as a basis for the development of a spacecraft radiometer for earth observations.

Reference 2 cites forecastings of agricultural production, management of land use and water resources as efforts that should be pursued. The Global Environment Program objectives (ref. 2) include monitoring, forecasting, and assessing global weather, air, and water quality. One method of global determination of these natural phenomena is through the usage of a Large Space Antenna (LSA) using microwave measurements.

One LSA concept being considered for development at Langley Research Center is the 122 m Hoop Column Antenna (HCA) shown in figure 1. This instrument will be a radiometer designed to detect electromagnetic radiation from Earth sources--soil and vegetation, at 1.4 GHz to infer their geophysical parameters. Electronic concepts for the acquisition and interpretation of these electromagnetic signals for the 122m HCA have been discussed in references 3, 4, and 5.

The concepts and analysis presented here provide information for the future development of the LSA radiometer concept. This paper will first present the geometric configuration required to house the detecting and processing electronics--the antennae feed network, for the 122 m HCA in a space environment. The housing which thermally isolates these components from the space environment, will be called the "radiometer container" for simplicity. Second, it will present the results of the thermal analysis of the radiometer containers with respect to their average surface temperature during four Earth orbits. And third, it will provide recommendations for extending the use of the analytical models for future studies.

RADIOMETER CONTAINER CONCEPTUAL CONFIGURATION

The operation of the 122 m Hoop Column Antenna (HCA) used as a radiometer is shown in figure 2. In this figure, electromagnetic radiation from Earth sources (soil and vegetation) is received by the antenna and converted into an electrical signal. This signal is then transmitted back to an Earth station for information processing. The basic concept for this radiometer was the Pushbroom Microwave Radiometer (PBMR) which was built and aircraft-tested at Langley Research Center. The thermal control work done in housing the radiometer is described in reference 1 and is the starting point for this paper in developing a geometric configuration for space application.

Three critical requirements had to be achieved with the PBMR: (1) the sensitive electronic components and the feed network of the radiometer had to be stable within $\pm 1.0^{\circ}\text{F}$ of a set temperature; (2) several integrated components of the electronic circuit had to be controlled within $\pm 0.1^{\circ}\text{F}$ about a set temperature; and (3) the active surface--i.e. the surface receiving the electromagnetic signal, had to be "radiometrically transparent." This meant that the active surface would have to be made of a material which would transmit the 1.4 GHz radiometric signal from Earth sources and reflect or emit little or no radiation at that frequency.

These same requirements are applicable to the 122 m HCA radiometer concept and in addition, (4) the instrument must be Shuttle compatible with respect to weight, stowability and deployability; and (5) the thermal control system must be as passive as possible because of limited solar battery power. Considering these five critical requirements, a data sheet was generated which defines the orbital, geometric, and thermal envelopes needed to develop the "radiometer container" concept.

Using constraints listed in Table 1, several radiometer container configurations for the electronic components were proposed in references 3 and 6. Figure 3 shows

the final concept which incorporates three separate radiometer containers to provide adequate field coverage.

Thermal control considerations for the proposed geometric configuration of the radiometer instrument is the goal of this project. However, in this paper, the determination of the surface temperature for the three radiometer containers in a low Earth orbit will be the first step in the development of the thermal control method.

Based on previous data (refs. 13, 14, and 15), multilayered insulation (MLI) composed of Kapton and fiberglass would be a viable concept for the radiometer containers for structural and thermal protection. Beneath the MLI, alternating layers of styrofoam and honeycomb separators thermally isolate the internal electrical components (fig. 4). The location of the active thermal control system which would provide set point control of $\pm 1.0^{\circ}\text{F}$ and $\pm 0.1^{\circ}\text{F}$ for selected electronic components, is also shown in figure 4. In addition, there are provisions for radiators if the container surfaces need to eliminate excess heat. This configuration would provide the structural integrity needed for strength and flexibility and thermal isolation for the radiometer components, while satisfying the radiometric transparency requirement. The radiometer instrument is to be equipped with solar batteries, however, the power available to operate auxiliary systems, such as an active thermal control system, would be small. For maximum passive thermal control, a thermal control coating could be applied to the MLI shell of the radiometer containers. Since a specific coating or radiometric properties--absorptivity (α) and emissivity (ϵ)--were not designated for the containers, a range of $(\alpha_s/\epsilon)^s$ ratios were studied.

The α_s/ϵ ratios were studied by modeling the container surfaces in an Earth orbit and obtaining their radiant heat loads. Those loads were then converted into container surface temperatures which dictated desirable α_s/ϵ ratios.

The description and results of the analysis comprise the remainder of this report.

THERMAL ANALYSIS

Solar, Earth, and albedo radiation are the three sources which heat the surfaces of the radiometer containers while in orbit.

Earth and albedo radiation inputs vary primarily because of the container's orientation in orbit with respect to the sun and weather patterns of the Earth's atmosphere (fig. 5). However, the radiation from the sun seen by the containers is approximately constant. Van Vliet (ref. 12) states that a satellite in Earth orbit absorbs solar and albedo radiation at wavelengths between 0.3 to 2 microns. The satellite also absorbs Earth radiation and emits its absorbed energy at wavelengths between 0.5 to 50 microns. Wavelengths in the region of maximum solar radiance account for the major heat inputs to the satellite while reradiation at longer wavelengths are significant for radiative cooling. The absorptance in the solar region is designated by α_s while ϵ represents the emittance at longer wavelengths. Passive thermal control is critically dependent on α_s/ϵ which serves to determine the surface temperature.

Kirchhoff's law states that the ratio of emissive power of a surface to its absorptance, at thermal equilibrium with its surroundings, is equal for all bodies

which suggests $\alpha/\epsilon = 1.0$. Also, Kirchoff's law states that at a specific wavelength, the absorptance and emittance are equal: $\alpha_\lambda = \epsilon_\lambda$.

For an orbital analysis, thermal equilibrium between the satellite and the space environment will not be achieved, thus $\alpha_{\lambda_1} T_1 \neq \epsilon_{\lambda_2} T_2$. Since solar absorptance of a satellite and its emittance are considered at different wavelengths (ref. 12),

$$\alpha_{\lambda_1} T_1 \neq \epsilon_{\lambda_2} T_1 \quad (\lambda_1 \neq \lambda_2)$$

in essence, Kirchoff's law is not violated.

Finally, the α_s/ϵ ratio for a surface or body in orbit can vary from 0.1 to 10 or more, depending on its thermal-optical properties.

In the analysis presented, the solar absorptance (α_s), of the radiometer containers, integrated over the solar wavelength spectrum is ratioed to the emittance (ϵ) at different wavelengths. The ratio was varied, with no specific coating indicated, and container surface temperatures were determined. A limited surface temperature range was then used to determine acceptable α_s/ϵ ratios for the selection of thermal control coatings.

Determination of the surface temperatures and properties for the three radiometer containers was done by implementing the following steps:

1. Defining the orbit for 122 m HCA.
2. Defining the specific geometry for each radiometer container and its orbital orientation to Earth and the sun.
3. Calculating the incident heat fluxes on each radiometer container for different α_s/ϵ ratios.
4. Calculating all surface temperatures for each container.
5. Plotting "average" surface temperature versus α_s/ϵ ratios.

Figure 6 shows the analysis tools and methods used to accomplish the five steps.

Orbit Definition.— Numerous mission tradeoffs were made for the 122 m HCA radiometer to determine orbital parameters for optimum radiometric performance. Definition of this optimum orbit included: (a) a low Earth orbit--666 km altitude, for optimum signal to noise ratio, (b) antenna inclination of 90-98° for pointing precision maximization, (c) a sun angle, β , of 90°, and (d) a continuous Earth facing orbit to optimize surface coverage. These parameters were calculated using a Langley Research Center-developed software package called "IDEAS"--Interactive Design and Analysis of Future Large Space Concepts (ref. 8), and they completely define the thermal environment for the analysis of the 122 m HCA.

Geometric Definitions.— Determination of the surface temperature of the three radiometer containers posed a special problem. The surface temperature is determined by calculating the incident heat flux on the containers from their exposure to potential radiation sources including Earth, deep space, and sun. The quantity of heat for each surface is dependent upon the thermal-optical properties of the surface, the source, and its projected surface area. This area is calculated by the

product of the total surface area and the cosine of the angle produced by the line-of-sight of the source, and the normal axis of the surface. In this case, the surfaces of all three containers are at skew and compound angles to any line-of-sight and the most casual effort to determine these areas would be a formidable task (figs. 4 and 7). Therefore, a three-dimensional computer model using ANVIL 4000, a computer aided-design (CAD) software package, was developed (ref. 9). This model shown in figure 7 depicts exact dimensions, geometric angles from the source (sun), line-of-sight, and volumes for the containers. Finally, using this model, the calculation of incident heat fluxes could be managed and directly related to all surfaces with consistency and accuracy.

Heat Flux Model.— Using the coordinates for the three radiometer containers generated by ANVIL 4000, the heat flux model was developed using Martin Marietta's Thermal Radiation Analyzer System software--TRASYS. The TRASYS model shown in figure 8, consisting of 28 nodes, represents all container surfaces. This model was used to determine the precise incident fluxes generated from orbital sources--sun, Earth, and deep space. Radiation exchange between radiometer containers was included in the calculation of heat fluxes; however, shadowing of containers by each other was considered minimal and was not included. Representative heat fluxes for the orbit definition and selected surfaces on the upper and lower left containers are presented in figures 9 through 15. It should be noted that the heat fluxes for the bottom left and right containers are similar; therefore, only the left is presented.

Surface Temperature.— The heat fluxes determined from the TRASYS model were used as inputs to a final computer model used to calculate container surface temperatures. This model was developed using a finite differencing program called MITAS--Martin Marietta Thermal Analysis System. The heat fluxes from TRASYS are converted by MITAS into input heating rates to the container surfaces. This heat input is then resolved into surface temperatures based on the material conductivities and the radiation factors between surface and sources. The total joule heating generated by the electronics would be 500 watts per container-- 3 watts/m^3 (0.09 watts/ft^3), and was considered a negligible internal heat source. The MITAS model shown in figure 16 consists of 28 diffusion nodes, 1 boundary node, 50 linear conductors, and 54 nonlinear radiation conductors.

Considering the quantity of data to be collected--5000 surface temperatures, and the fact that the fluxes (heat input) experienced by the bottom "left" and "right" containers are the same, symmetry was employed to reduce the quantity of data needed. Therefore, the "top" and "bottom left" radiometer containers will be used for the surface temperature study.

An initial study was made for the radiometer containers in orbit to roughly estimate the temperature levels they would experience. This study did not include radiation exchange between containers and radiation from sources was assumed to be maximum. The results of this initial "look" indicated that the container surfaces with an absorptance of 0.5 and an emittance of 0.9, thus $\alpha_s/\epsilon \sim 0.6$, would not exceed the -4°F to 150°F range for the enclosed electronics. The surface temperature of the sun facing surfaces, however, did exceed the temperature range and was attributed to their full sun-to-full shadow exposure during orbit. Finally, an "average" container temperature was calculated for each container and this temperature was within the temperature limits of the electronic components.

At this point in the analysis, it was clear that a decision would have to be made whether all surface temperatures for each container be evaluated individually or an "average" container surface temperature be used. It was decided in the interest

of simplicity and ease of discussion, the "average" container surface temperature concept would be used. This method would bracket the available choices of α_s/ϵ ratios for each radiometer. Specific surface temperatures could then be examined for each radiometer container to ensure compliance with design requirements. Therefore, a study of the α_s/ϵ ratios and its effect on the "average" container surface temperature was conducted.

The radiometer containers--"top" and "bottom left," were simulated through four orbits around Earth using the complete MITAS thermal model shown in figure 16. Four orbits were selected to ensure that the containers would reach a stable thermal level. The α_s/ϵ ratios examined would range from 0.1 to 5.0. Since either absorptivity or emissivity can be varied, it was decided that the absorptivity would be changed from 0.1 to 0.9. Figure 17 shows all the possible α_s/ϵ ratios and the ones selected for this study.

The reasoning used for selecting the indicated α_s/ϵ ratios shown in figure 17 is as follows. The initial study conducted for the radiometer containers using an absorptance of 0.5 and an $\alpha_s/\epsilon = 0.6$ served as a starting point for the examination of the complete MITAS model. For this absorptance, $\alpha_s = 0.5$ other α_s/ϵ ratios--0.7, 1.0, 2.0, and 5.0 were explored. Finally, in order to obtain a clearer picture of the containers surface temperatures other absorptances were examined for various α_s/ϵ ratios. This examination covered absorptances from 0.1 to 0.9 and included α_s/ϵ ratios from 0.1 to 5.0.

For each α_s/ϵ ratio selected, all surface temperatures were obtained through the MITAS model. Then, an "average" surface temperature for each container was calculated to judge the validity of the selected α_s/ϵ ratio. A "weighted" average surface temperature was adopted and was defined as

$$TAVG = \frac{\sum_{i=1}^n T_i A_i}{\sum_{i=1}^n A_i} \quad \text{where } n = 6; \text{ for "top" container} \quad (1)$$

$$n = 7; \text{ for "bottom" container}$$

T_i is a surface temperature at a specified time in each orbit, A_i is the area of that surface, i represents the specific surface of a container, and n the number of surfaces for a specific container. In each of the four orbits, at consistent times, the maximum and minimum temperatures were obtained for each surface and put into equation (1). These temperatures--TAVGMAX and TAVGMIN--were then plotted against the α_s/ϵ ratios to create a tool for selecting surface properties for the radiometer. Since the temperature envelop for the enclosed electronic equipment was -4°F to 150°F , it was arbitrarily decided that the temperature limits used to evaluate the α_s/ϵ ratios would be 0°F minimum and 100°F maximum.

RESULTS

Graphic representation of the "average" container surface temperatures for the "top" and "bottom" radiometers are presented. These temperatures were calculated at various α_s/ϵ ratios. Finally, a summary is presented demonstrating the use of the surface temperature vs. α_s/ϵ ratio curves.

Top Radiometer Container.- In figure 18, we see that for absorptances of 0.1 through 0.4, the average surface temperature envelop for the top radiometer container is from 20°F to -100°F and below. The criteria used for selecting a desirable α_s/ϵ ratio, is that both TAVGMAX and TAVGMIN surface temperatures must be above the minimum electronic component temperature limit of 0°F. In figure 18, the surface temperature criteria is not met, therefore, no α_s/ϵ ratio is selectable for absorptances from 0.1 to 0.4.

In figure 19 for absorptances of 0.5 through 0.9, the surface temperature envelop is from 80°F to -60°F. TAVGMAX and TAVGMIN surface temperatures for α_s/ϵ ratios from 1.0 to 2.0 straddle the minimum component temperature limit and for α_s/ϵ ratios from 2.0 to 5.0 are below the minimum temperature limit. Therefore, α_s/ϵ ratios from 1.0 to 5.0 are unacceptable. However, α_s/ϵ ratios from 0.6 to 1.0 produce average surface temperatures that fall within the maximum and minimum component temperature limits. Therefore, absorptances of 0.5, 0.6, 0.7, 0.8, and 0.9 are acceptable and can be considered in defining thermal properties for the "top" radiometer container.

Bottom Left (Right) Radiometer.- In figure 20 we see that the container average surface temperatures for α_s/ϵ ratios 1.0 through 5.0 do not meet the criteria of being above the minimum component temperature limit, therefore, absorptances from 0.1 to 0.4 do not qualify for consideration.

In figure 21, α_s/ϵ ratios from 0.6 to 1.0 produce average surface temperatures that meet the criteria and absorptances of 0.5, 0.6, 0.7, 0.8, and 0.9 can be considered in defining the thermal properties for the "bottom" left radiometer container. Symmetry of the bottom left and right radiometer containers, eliminates the need to analyze both containers. The temperatures, α_s/ϵ ratios, and acceptable absorptances apply for both containers.

CONCLUSION

Figure 22 shows the thermal regions where selectable absorptances, for maximum or minimum surface temperatures of the "top" radiometer container, can be found. These regions are bound by the minimum component temperature limit, the α_s/ϵ ratio range--0.6 to 1.0, and the maximum "average" surface temperature for each absorptance value--0.5, 0.6, 0.7, and 0.9. Using these regions and absorptance contour lines, the surface properties of the "top" radiometer container can be determined. For example, if an "average" surface temperature of 20°F was selected for this container, an $\alpha_s = 0.5$ would be chosen for the highest expected surface temperature. An $\alpha_s = 0.9$ would be available for the lowest expected surface temperature. From the intersection of the selected temperature and the absorptivity contour line, an α_s/ϵ ratio is defined and thus emittance. Figures 23A and 23B indicate the thermal regions and absorptance contours for the "bottom" radiometer containers. Once the properties are defined for each container, selection for the proper surface coating or texture can be conducted.

Recommendations.- The investigation undertaken in this paper provides a starting point for future, detailed analysis of the 122 m HCA radiometer concept. Once a desired operating temperature for the enclosed electronics is chosen, several avenues should be explored:

1. Examination of the specific container surfaces.- The average surface temperature obtained in this paper simply specifies all surface properties as equal.

As seen in the initial study, the sun facing surface experiences larger temperature swings, therefore, special attention should be given to this surface. The other surfaces should be well within the temperature limits using the technique developed in this paper.

2. Inside wall surface temperature.- Once the outside surface temperatures are determined, further study of the inside wall temperatures will define the thickness of the container skin and the thickness of the honeycomb isolators. In addition, the knowledge of the inside surfaces will determine if radiators or heat pipes are needed for thermal transport of heat buildup.

3. Comparison tests.- The results from these detailed studies should then be compared with thermal testing data to insure survivability of the thermal coatings or textures selected.

Execution of the above recommendations would complete the work started here in designing the 122 m Hoop Column Antenna Radiometer containers.

Langley Research Center
National Aeronautics and Space Administration
Hampton, Virginia
August 1986

REFERENCES

1. Dillon-Townes, Lawrence A.; and Averill, Robert, D.: Thermoelectric Temperature Control System for the Pushbroom Microwave Radiometer (PBMR), NASA TM-85824, June 1984.
2. Keafer, Lloyd S., Jr.; and Harrington, Richard F.: Radiometer Requirements for Earth-Observation Systems Using Large Space Antennas, NASA Ref. Publication 1101, June 1983.
3. Bailey, M. C.: Preliminary Design of 19-Element Feed Cluster for a Large F/D Reflector Antenna NASA TM-815666, August 1983.
4. Harrington, Richard F.; and Hearn, Chase P.: Microwave Integrated Circuit Radiometer Front-Ends for the Pushbroom Microwave Radiometer, Government Microcircuit Applications Conference, Orlando, FL, November 2-4, 1982.
5. Harrington, Richard F.: The Development of a Stepped Frequency Microwave Radiometer and Its Application to Remote Sensing of the Earth, NASA TM-81847, June 1980.
6. Foldes, Peter: 122m Hoop Column Antenna Radiometer Triplet Feed Concepts, NOTES, Folders Inc., 1983.
7. Large Space Systems Technology, NASA CP-2215, Volume 2, 1981.
8. Garrett, L. Bernard: Interactive Design and Analysis of Future Large Space Concept, NASA TP 1937, December 1981.
9. Anon: ANVIL 4000 Users Manuals Release 1, Manufacturing and Consultant Services, Inc., 9500 Toledo Way, Irvine, California 92718.
10. Goble, R. G.; and Jensen, C. L.: TRASYS II, Thermal Radiation Analysis System, Revision 2.0, Users Manual, NASA CR-159273-1, June 1980.
11. Anon: MITAS II, Martin-Marieta Interactive Thermal Analysis System Version 2.0, Users Manual, Martin-Marietta, Report M-76-2, May 1976.
12. Van Vliet, Robert: Passive Temperature Control in the Space Environment, MacMillan Co., NY, 1965.
13. Kimmel, B. G.: Development of Dielectric Windows for Spacecraft, NASA CR-53400, September 1963.
14. Campbell, T. G.: Summary of Antenna Technology at the Langley Research Center, NASA Conference Publication 2215, Part 2, Large Space Systems Technology - 1981, pp. 491, 503, and 711, November 16-19, 1981.
15. Metalized Products Division of King-Steeley Thermos Company, Winchester, Massachusetts, NRC-2, Super Insulation Product Sheet, 5-81-2M.

Bibliography

1. Brogren, E. W.; Barclay, D. L.; and Straayer, J. W.: Simplified Thermal Estimation Techniques for Large Space Structures, NASA CR-14523, October 1977.
2. Ewen, H. I.: State of the Art Microwave and Millimeter Wave Radiometric Sensors, Proceedings of the Symposium on Electromagnetic Sensing of the Earth from Satellites, Polytechnic Press of the Polytechnic Institute of Brooklyn, 1965.
3. Kendall, Bruce M.: Passive Microwave Sensing of Coastal Area Waters, AIAA paper #80-1953, AIAA conference on Sensor Systems for the 80's, December 2-7, 1980.
4. Blume, Hans-Juergen, C.; Kendall, Bruce M.; and Fedors, John C.: Sea-Surface Temperature and Salinity Mapping from Remote Microwave Radiometric Measurement of Brightness Temperature. NASA TP-1077, December 1977.
5. Barclay, D. L.; Brogren, E. W.; Fosth, D. C.; Gates, R. M.; and Straayer, J. N.: Large Space Structures Configuration, Packaging, and Response Studies, NASA CR-158928, September 1978.
6. Cushman, J. B.; and McCleskey, S. F.: Design Allowables Test Program, Celion 3000/PMR-15 and Celion 6000/PMR-15, Graphite/Polymide Composites," NASA CR-165840, June 1982.
7. Paus, J. R.: Carbon Fiber Composites, Reprint From Design News, Technologies for the 80's, July 6, 1981, Cahners Publication.
8. Ferebee, Melvin J.; Wright, Robert L.; and Farmer, Jeffrey: Weight and Structural Analysis of Four Structural Concepts for a Land Mobile Satellite System" SAWE paper #1456, index category #24, Society of Allied Weight Engineers, Inc., Conf., May 17-19, 1982.
9. Holloway, P. F.; and Garrett, L. Bernard: Comparative Analysis of Space-to-Space Central Power Stations. NASA TP-1955, December 1981.
10. Gilreath, Melvin C.; and Castellow, Stark L., Jr.: High-Temperature Dielectric Properties of Candidate Space-Shuttle Thermal Protection System and Antenna-Window Materials. NASA Technical Note TN-D-7523, June 1974.
11. Kuhlman, E. A.: Development of S-Bond Antenna Interface Design, NASA CR-147716.
12. Marchetti, M.; and Marganti, F.: Prediction of Thermal Expansion Coefficients of Sandwiches Using Finite Element Method, Validated by Experimental Test Results, IAF Paper 82-383, September 1982.
13. Adelman, H. M.; and Shore, C. P.: Thermal Analysis Considerations for Large Space Structures, NASA CP-2258, February 1983.
14. Composite Reliability, ASTM Special Technical Publication 580, April 5-16, 1974, AIAA Conference.

15. Fager, J. A.: Application of Graphite Composites to Future Spacecraft Antennas, AIAA Paper 76-238, April 1976.
16. Dharan, C. K. H.: Mechanical and Thermal Behavior Characterization of Composite Materials for Communications Spacecraft, Conference on Composite Materials, Metallurgical Society of AIME paper #A79-16981 05-24, April 16-20, 1978.
17. Chalmers, D.: In-Orbit Degradation of Thermo-Optical Material Properties on OTS-2, SAE paper 820863, July 19-21, 1982.
18. Franklin, James L.; and Kramer, Ted J., Thermal Design of Standard Avionic Enclosures, SAE paper 820878, July 19-21, 1982.
19. Bouchez, J. P.; and Bussolino, L.: Study and Design of a Heat Rejection System for Advanced Spacecraft and Payload Thermal Control," SAE paper 820845, July 19-21, 1982.
20. Nervegna, N.; and Borio, U.: A Finite Element Thermal Modelling of Modular Space Radiators, SAE paper 820865, July 19-21, 1982.
21. Marchis, V.: Control Philosophy Concepts in Complex Space Heat Rejection Systems, SAE 820864, July 19-21, 1982.
22. Vallerani, E.; Liroy, S.; and Sessions, B.: Thermal Concepts Derived From Spacelab for Advanced Space Stations/Platforms, SAE 8208162, July 19-21, 1982.
23. Lyle, Robert; Stabekis, Pericles; Stroud, Robert: Spacecraft Thermal Control, NASA SP-8105, May 1973.
24. Brooks, D. R.: An Introduction to Orbit Dynamics and Its Application to Satellite-Based Earth Monitoring Missions, NASA RP-1009, November 1977.
25. Neubert, H. D.: Thermally Inert Composite Hardware Applications for Spacecraft, SAMPE Journal, Vol. 14, May-June 1978, p. 6-14.

Orbital, Geometric, and Thermal Data
for the Radiometer Container

Orbital Data+

- Altitude: 666 km; low Earth orbit
- Orbit plan inclination: 90° - 98°
- Antenna orientation: Earth oriented
- Mission duration: 3 years
- Orbit type: polar
- Beta angle (sun angle): 90° [angle of sun line-of-sight to Earth's axis]

Geometric Data

- Radiometer container envelope*; 15.5 m x 3.5 m x 0.3 m
- Container weight++; 977 kg; 244 kg/container
- Internal electronics and thermal instruments*:
 - receiver array and p. c. boards
envelope: 15.0 m x 3.0 m x 0.05 m
weight: 700 kg
 - electronic and thermal systems
envelope: 15.0 m x 3.0 m x 0.15 m
weight: 120 kg

Thermal Data

- Electronic components: max 150°F
min -4°F
- Dissipated power per container: 500 watts
- Container material: Kapton-fiberglass
multi-layered insulation;
"radiometrically transparent"
- Container surface absorptance and emittance: TBD

+ref. 2
*ref. 6
++ref. 7

Table 1.- 122 m radiometer container design data.

ORIGINAL PAGE IS
OF POOR QUALITY

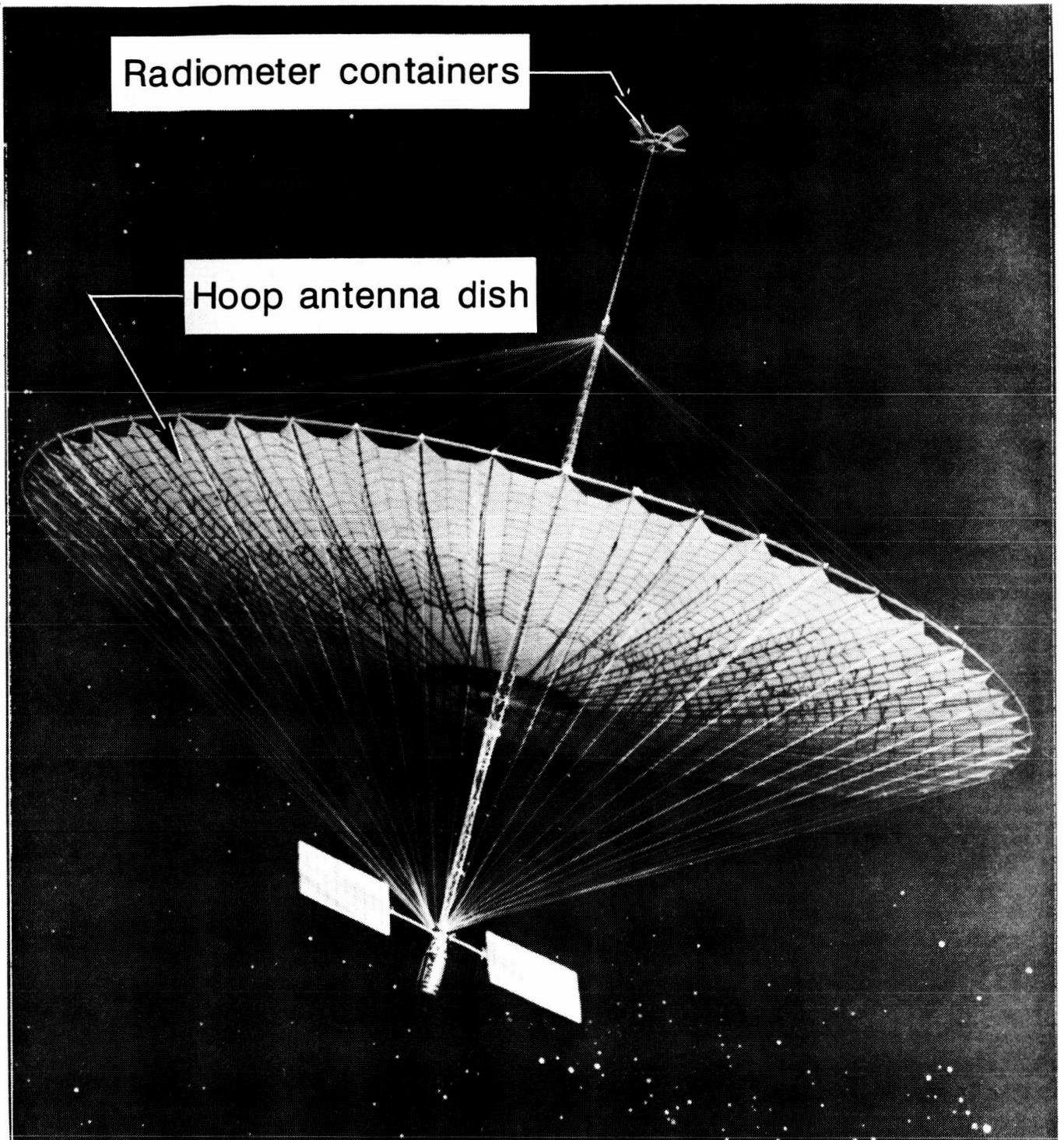


Figure 1. - 122m Hoop Column Concept.

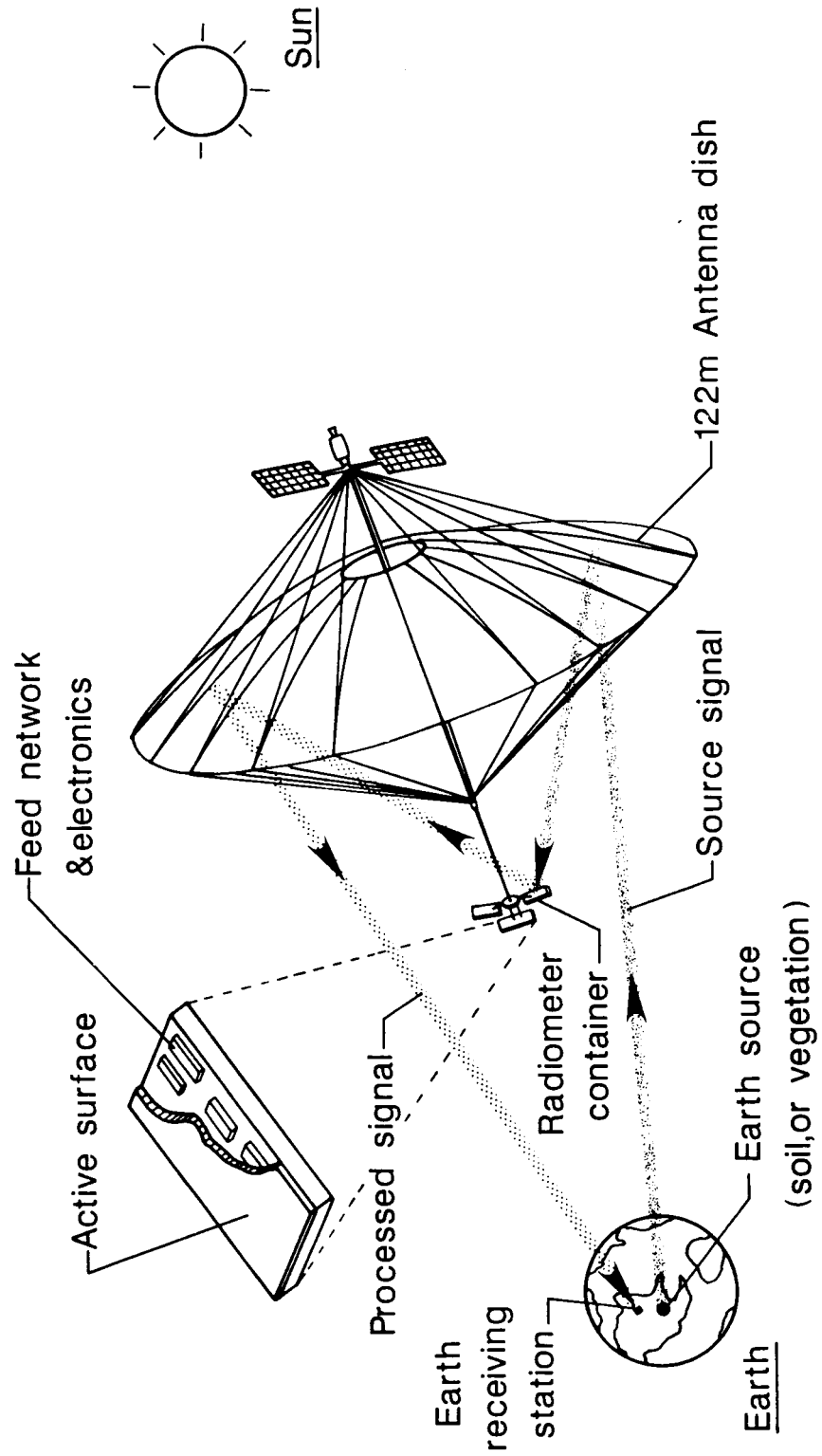


Figure 2. - 122m radiometer operation for sensing geophysical parameters.

ORIGINAL PAGE IS
OF POOR QUALITY

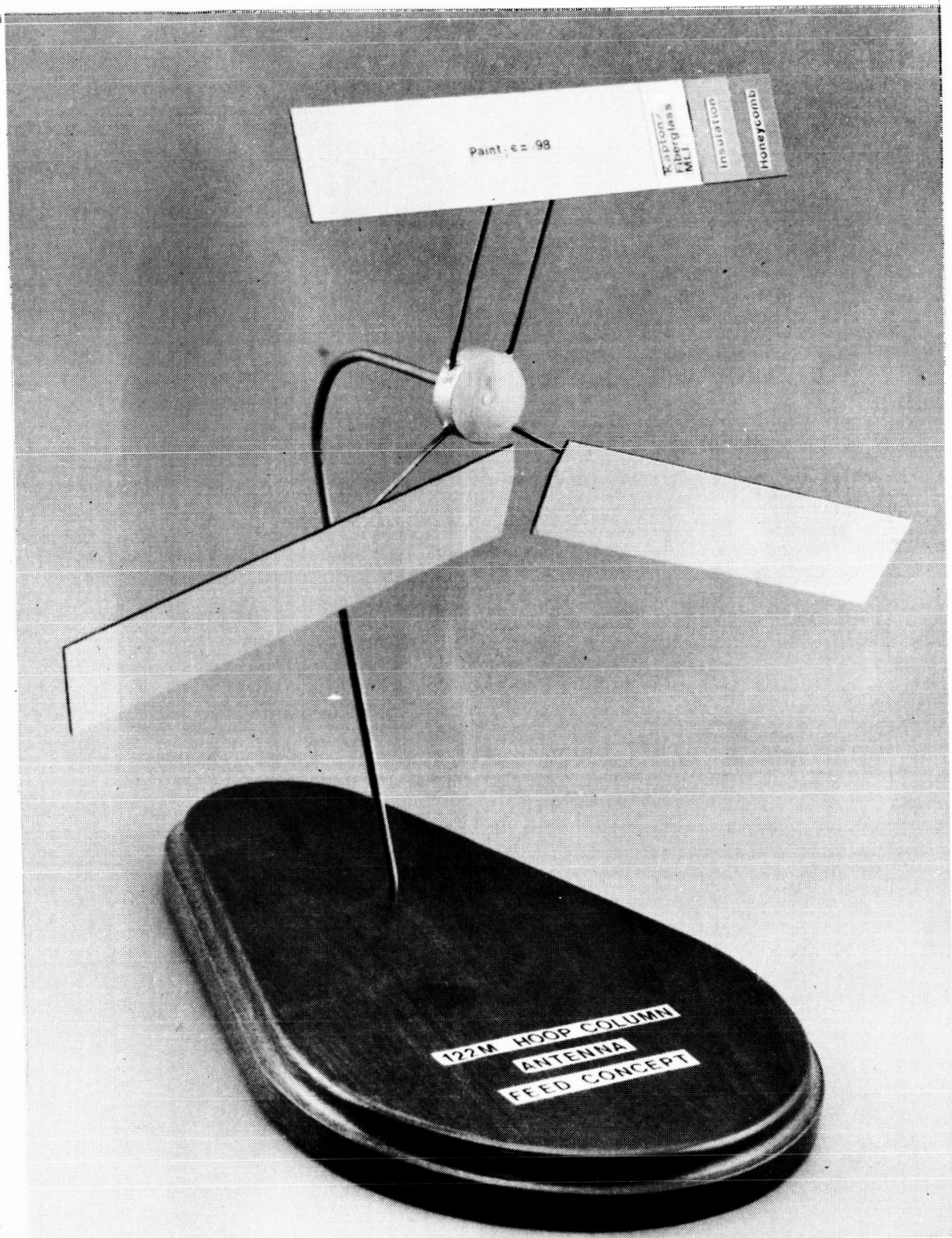


Figure 3. - 122m Hoop Column radiometer concept.

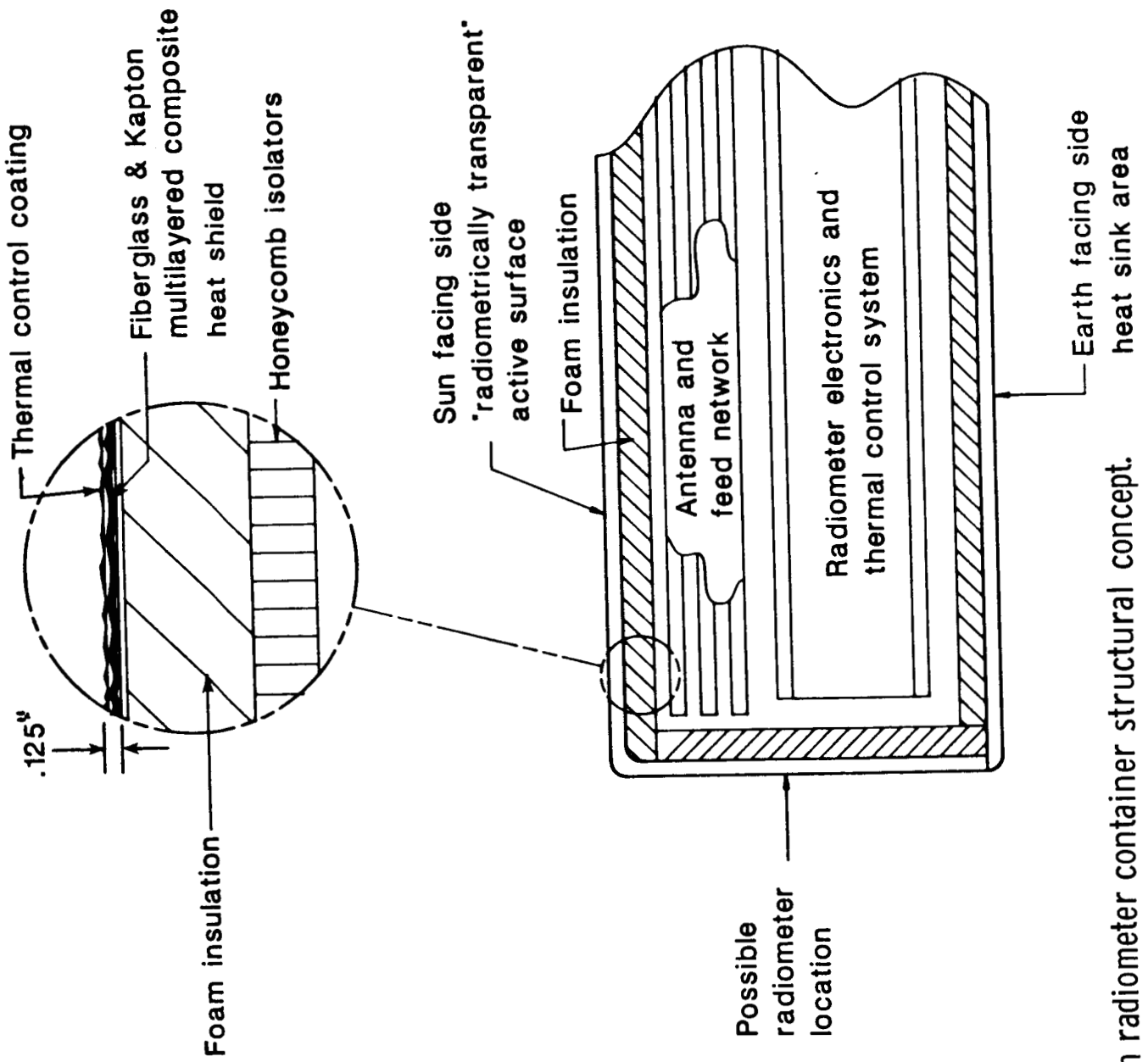


Figure 4. - 122m radiometer container structural concept.

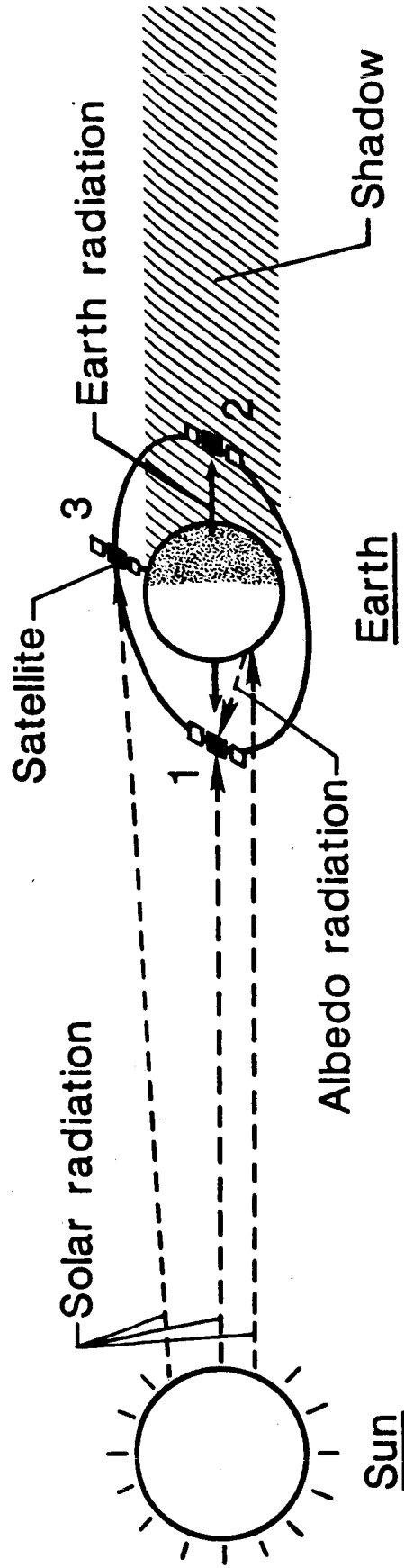


Figure 5. - Satellite thermal inputs in Earth orbit.

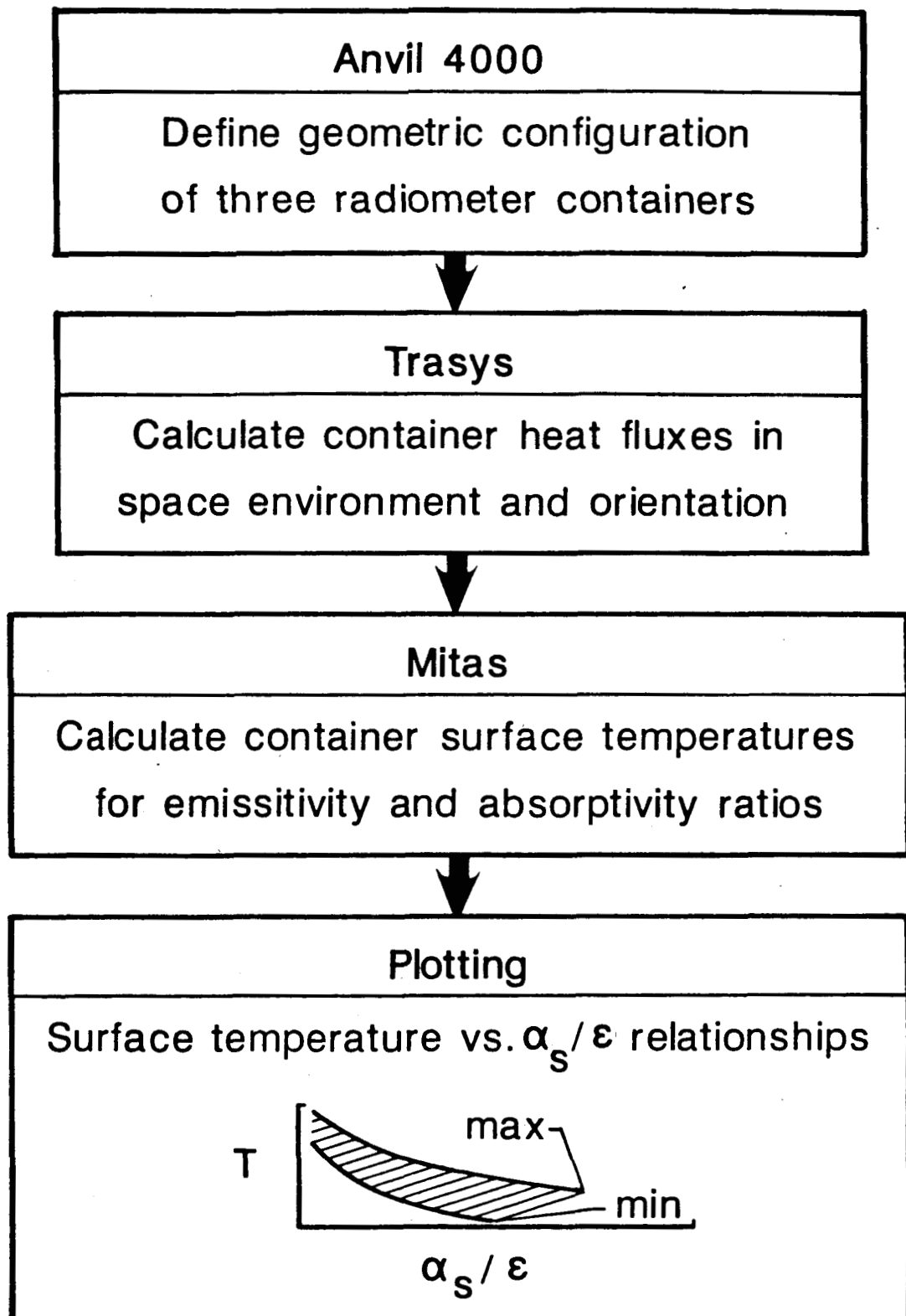


Figure 6. - Thermal analysis flow chart.

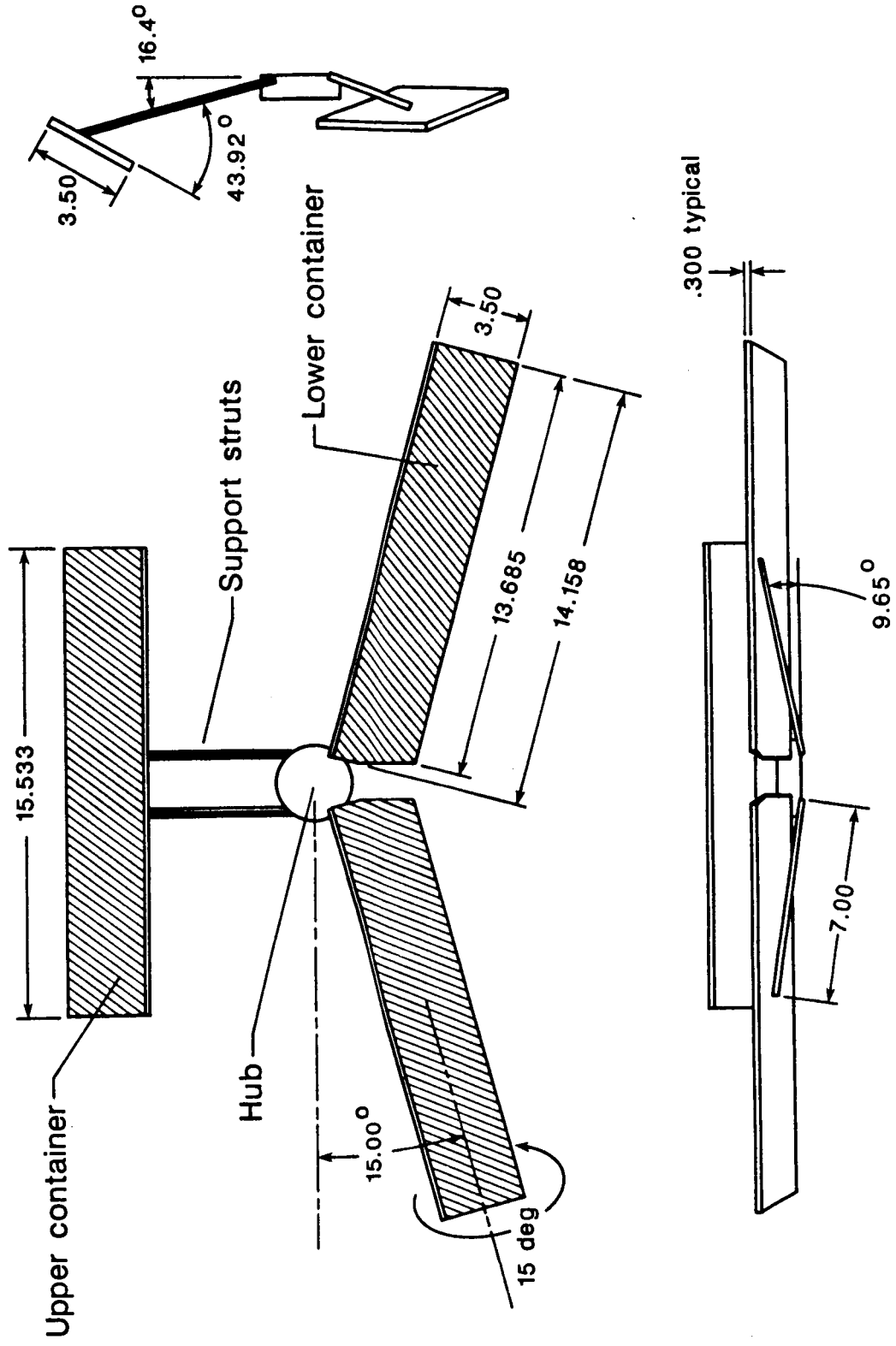


Figure 7. - ANVIL 4000 computer generated model of three radiometer containers for 122m HCA.

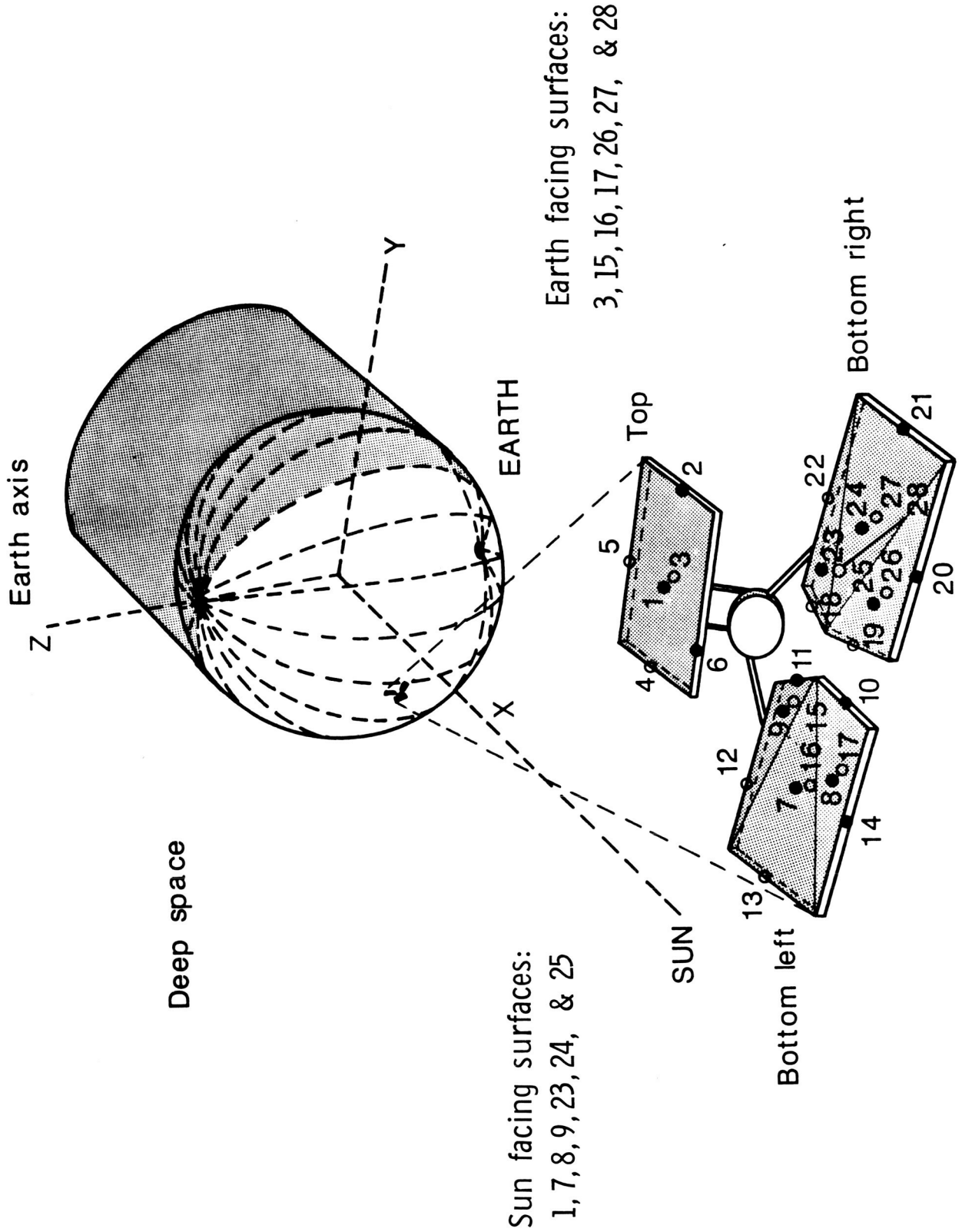


Figure 8. - 122m HCA TRASYS model.

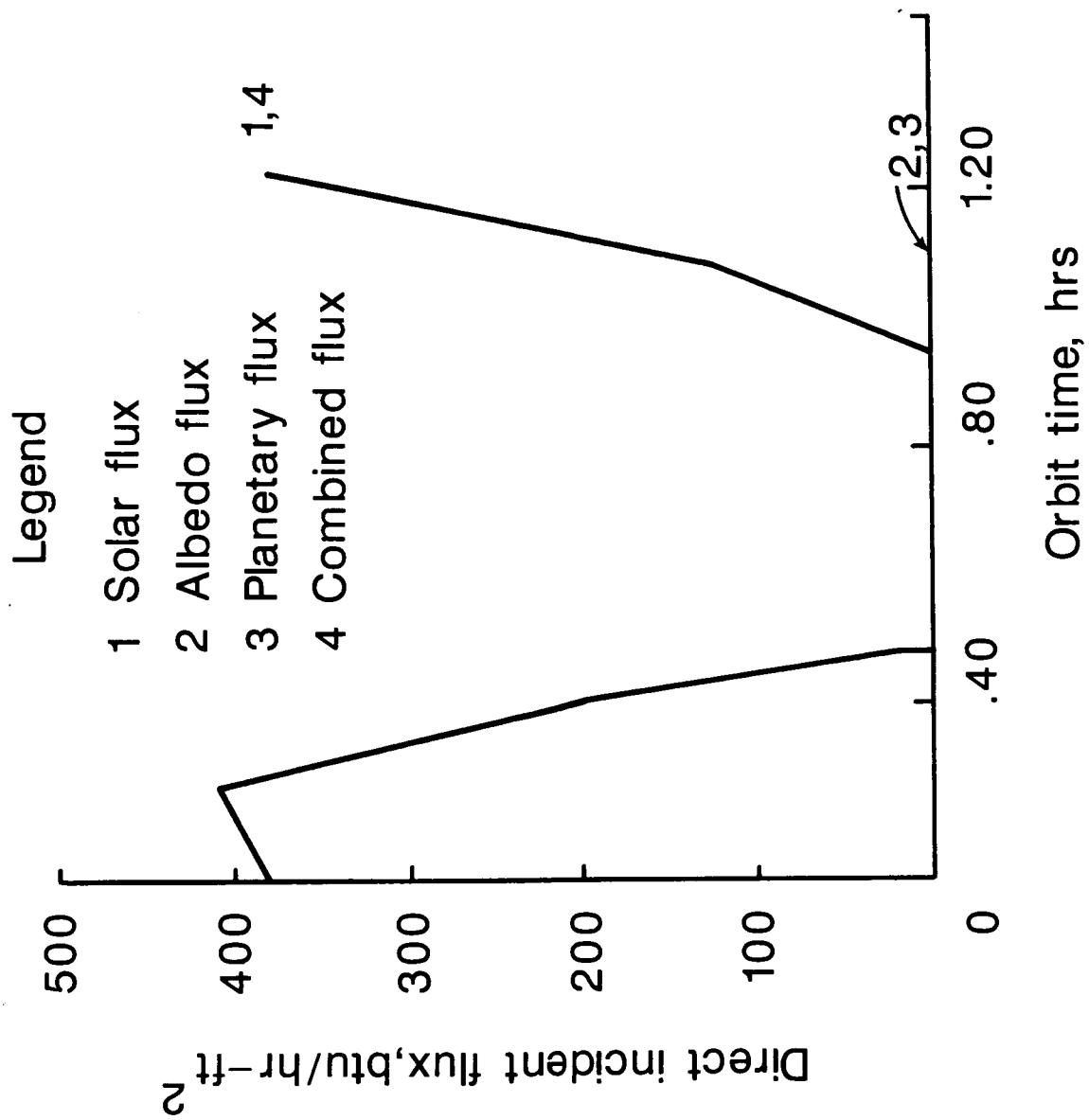


Figure 9. Heat fluxes for surface 1; top radiometer container
 $\alpha_s = .5$, $\epsilon = .9$, $\beta = 90^\circ$; sun facing surface

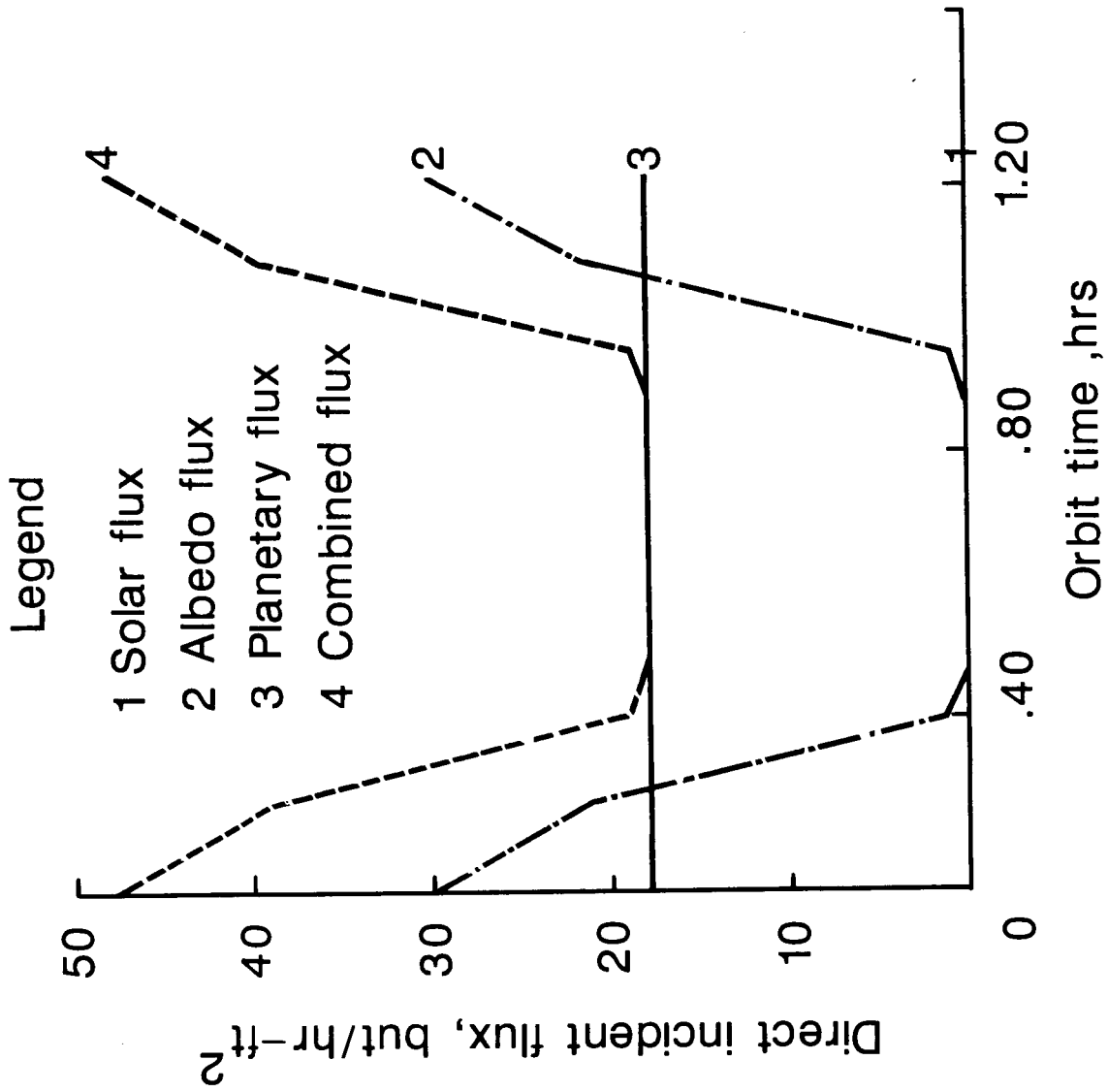


Figure 10. Heat fluxes for surface 2; top radiometer container
 $\alpha_s = .5, \epsilon = .9, \beta = 90^\circ$; edge

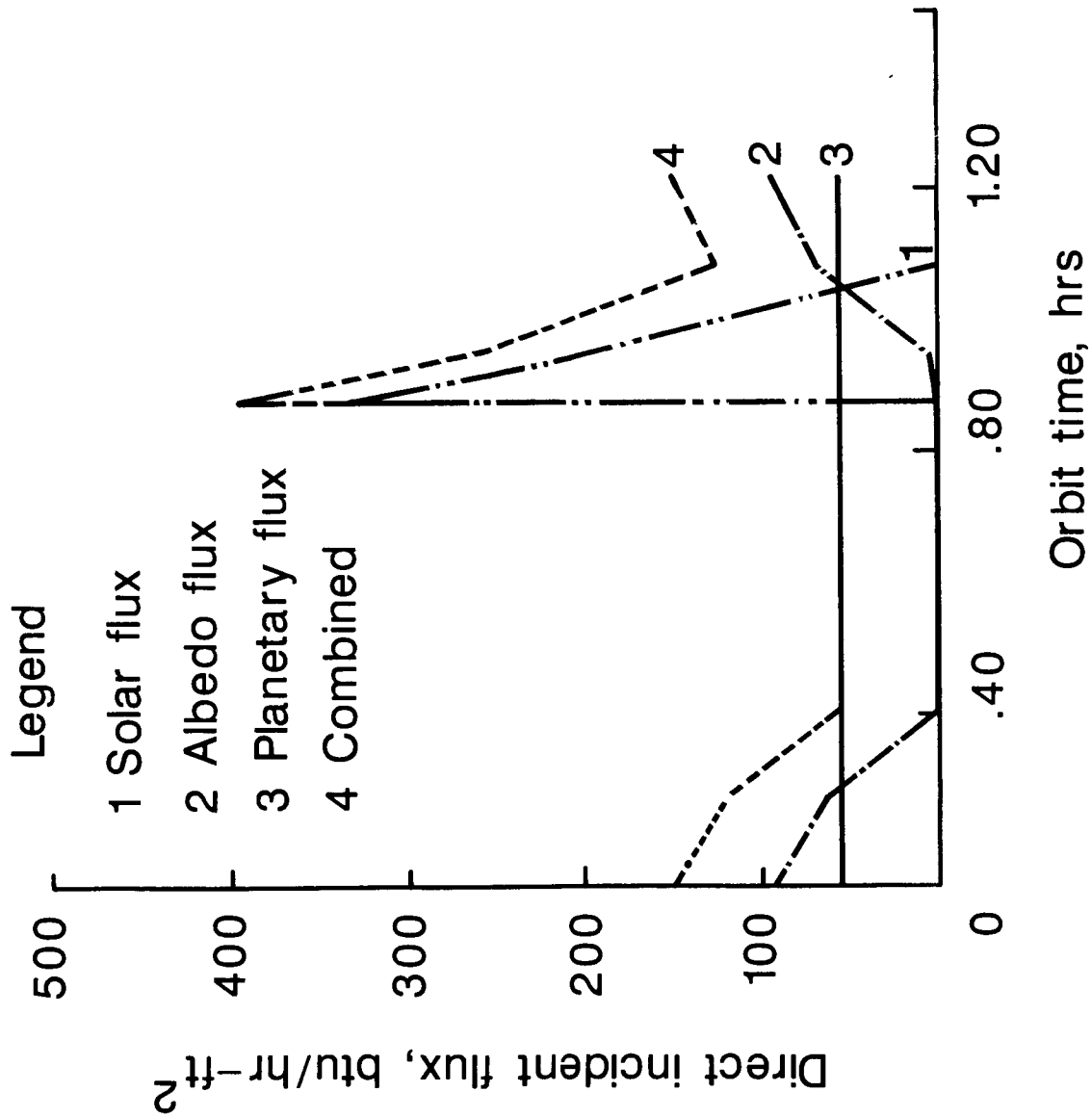


Figure 11. Heat fluxes for surface 3; top radiometer container
 $\alpha_s = .5$, $\epsilon = .9$, $\beta = 90^\circ$; edge

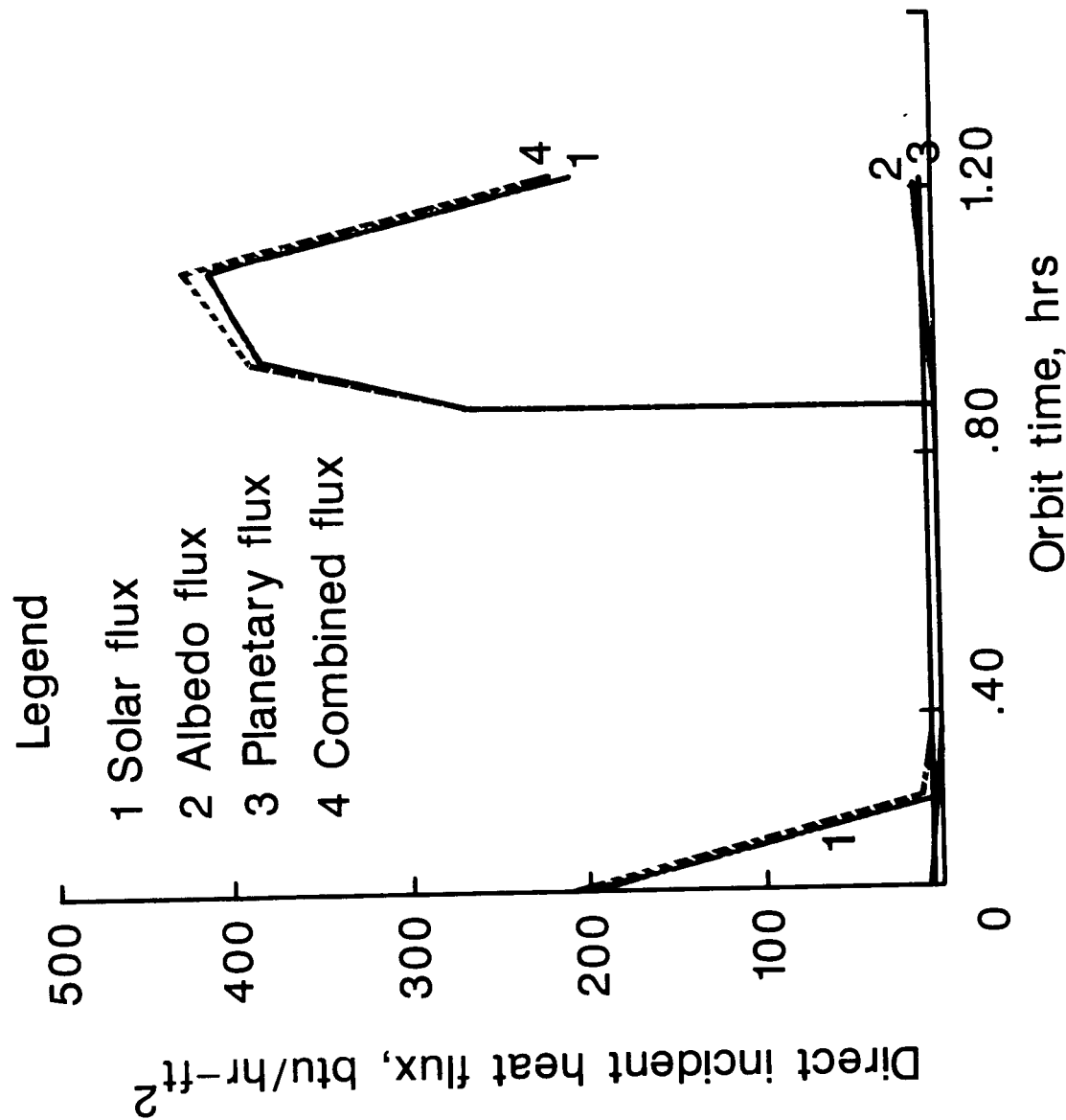


Figure 12. Heat fluxes for surface 6; top radiometer container
 $\alpha_s = .5, \epsilon = .9, \beta = 90^\circ$

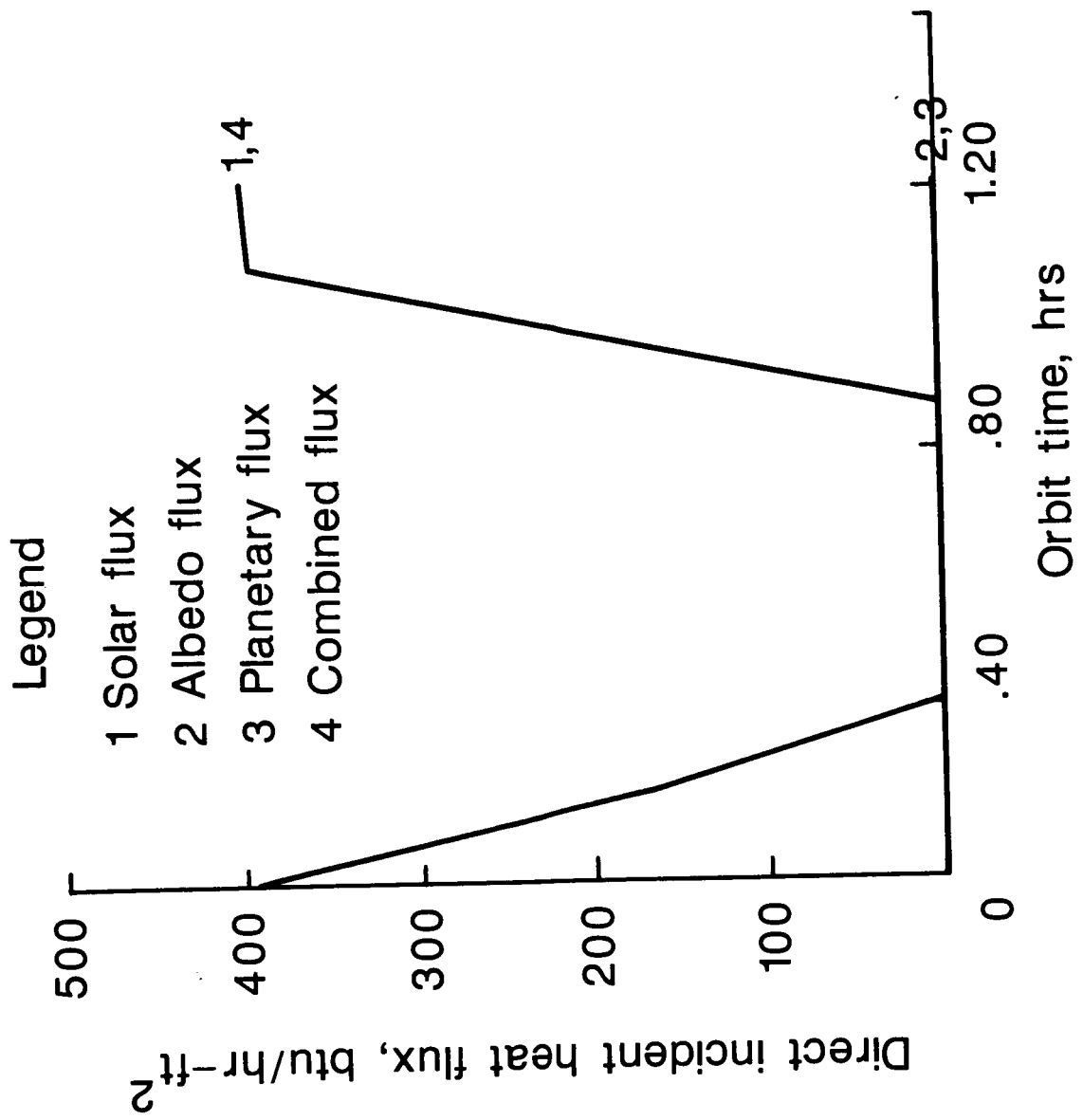


Figure 13. Heat fluxes for surface 12, bottom radiometer container
 $\alpha_s = .5, \epsilon = .9, \beta = 90^\circ$; edge

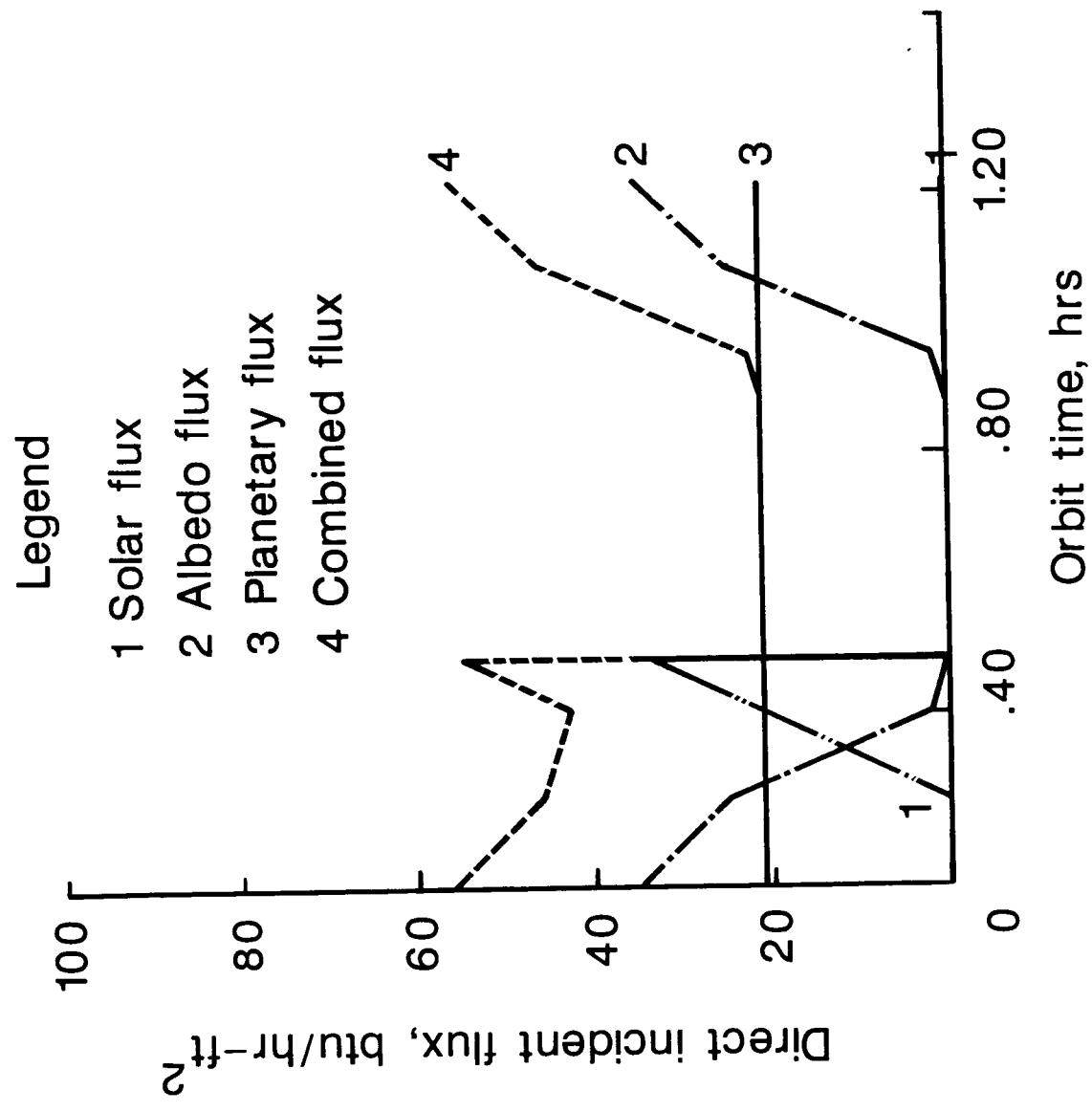


Figure 14. Heat fluxes for surface 10; bottom radiometer container $\alpha_s = .5$, $\epsilon = .9$, $\beta = 90^\circ$; edge

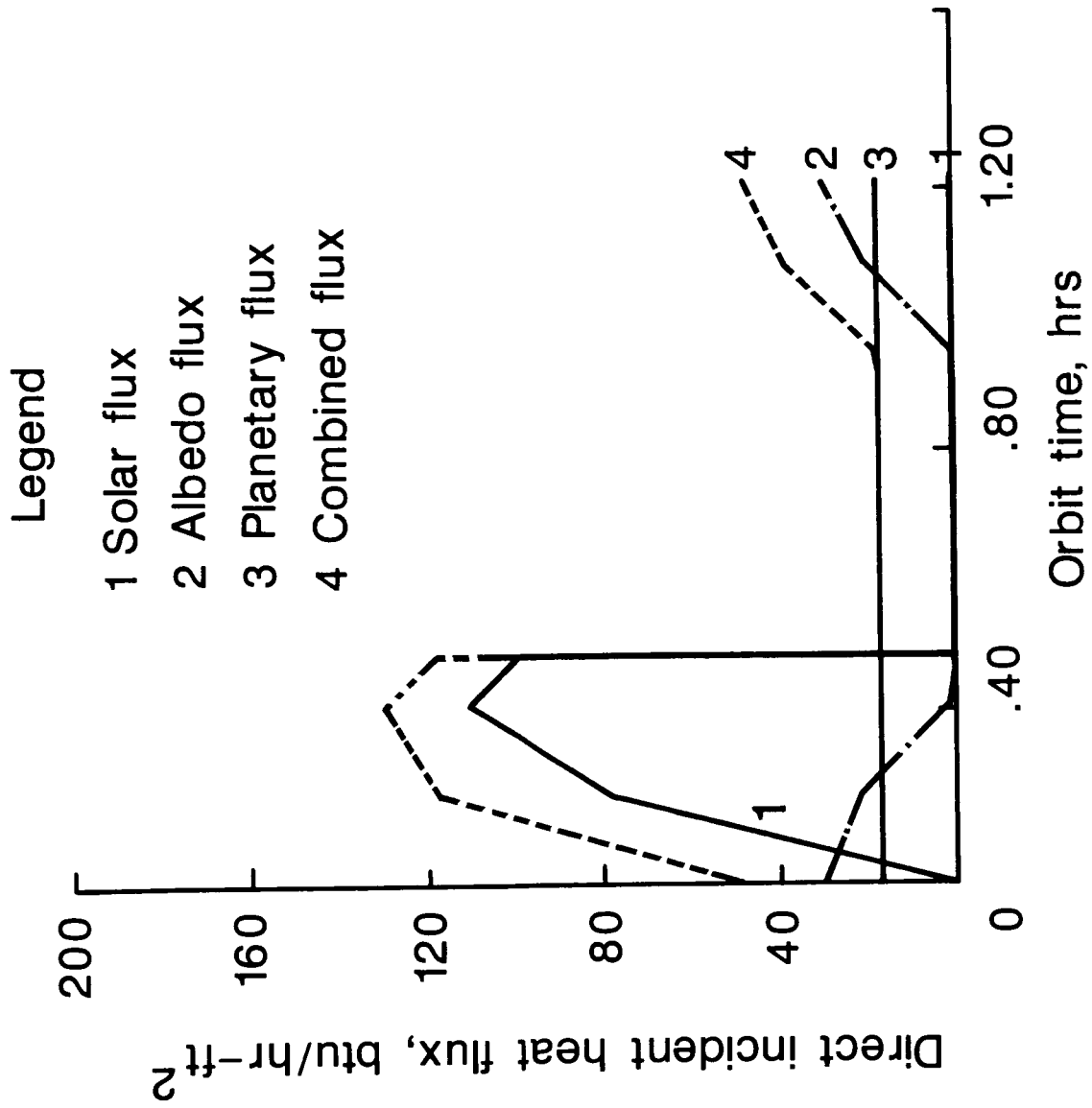
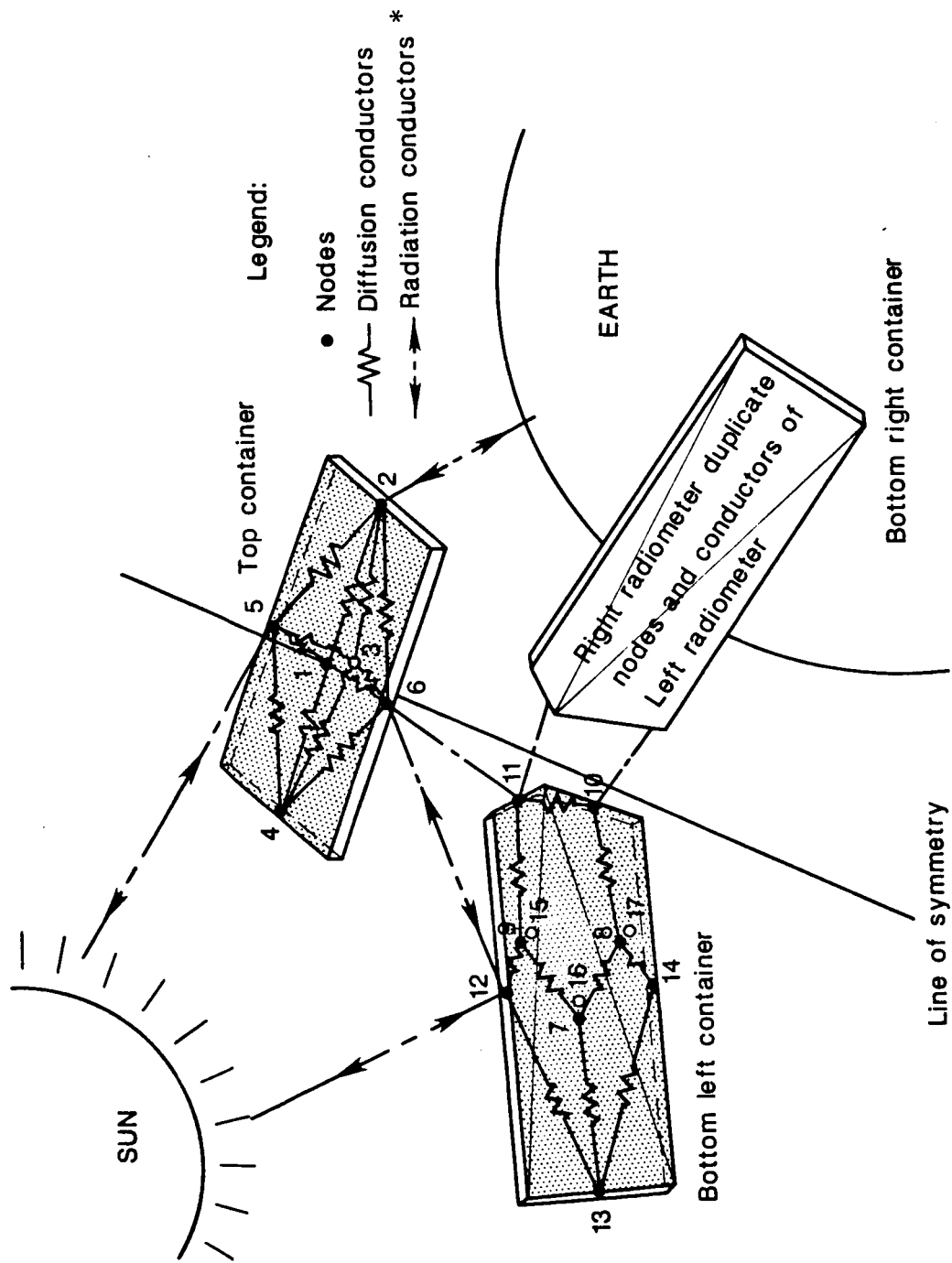


Figure 15. Heat fluxes for surface 11; bottom radiometer container $\alpha_s = .5$, $\epsilon = .9$, $\beta = 90^\circ$; edge



* All radiation conductors are not shown to reduce confusion

Figure 16. 122m HCA radiometer MITAS thermal model

		Emittance, ϵ								
		.1	.2	.3	.4	.5	.6	.7	.8	.9
Absorptance, α	.1	1	.5	(.3)	.2	.2	(.2)	.1	.1	(.1)
	.2	2	1	.7	.5	.4	.3	.3	.2	.2
	.3	3	2	1	.8	.6	.5	.4	.4	.3
	.4	(4)	2	1	1	.8	.7	.6	.5	(.4)
	.5	(5)	2	(2)	1	(1)	.8	.7	.6	(.6) ← Initial Study
	.6	6	(3)	2	(2)	1	(1)	.9	.8	(.7)
	.7	7	4	2	(2)	1	1	1	.9	(.8)
	.8	8	4	3	2	2	1	1	1	.9
	.9	9	4	3	2	2	(2)	1	1	1

Figure 17.- Absorptance vs. emittance, α_s/ϵ ratio table

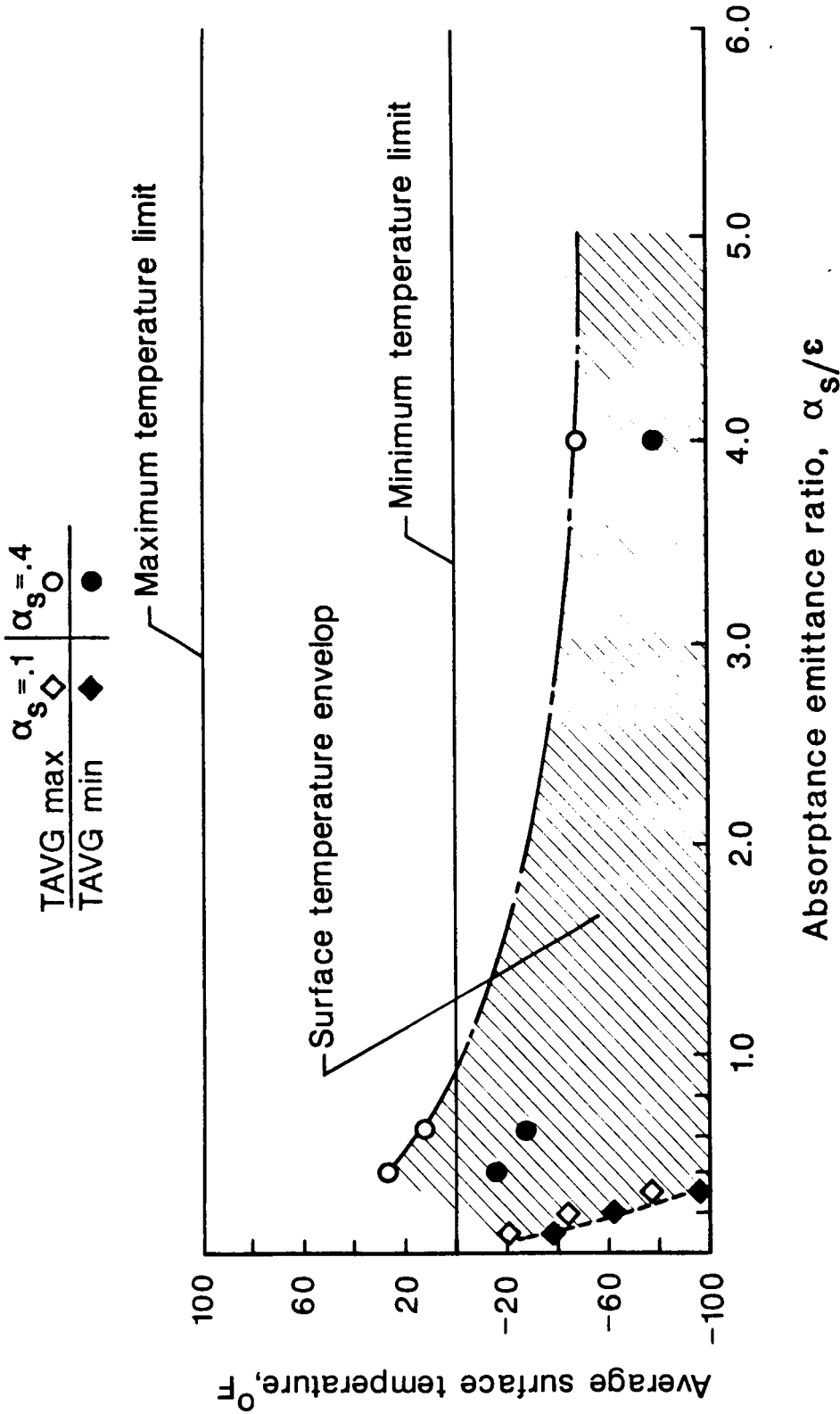


Figure 18. - Average surface temperature envelop for "top" radiometer container; $\alpha_s = 0.1$, and 0.4.

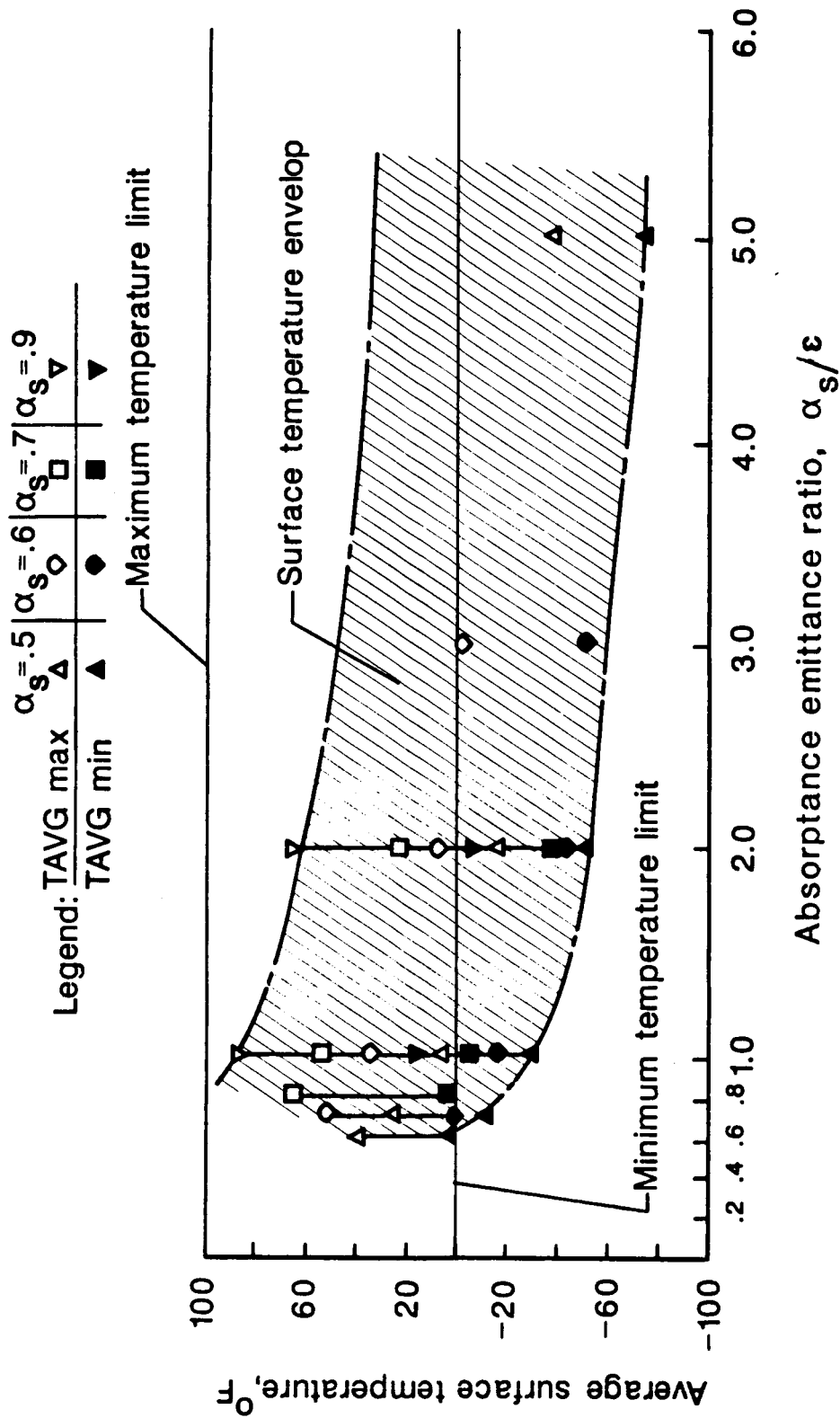


Figure 19. - Average surface temperature envelope for "bottom" radiometer container, $\alpha_s = 0.5, 0.6, 0.7, \text{ and } 0.9$.

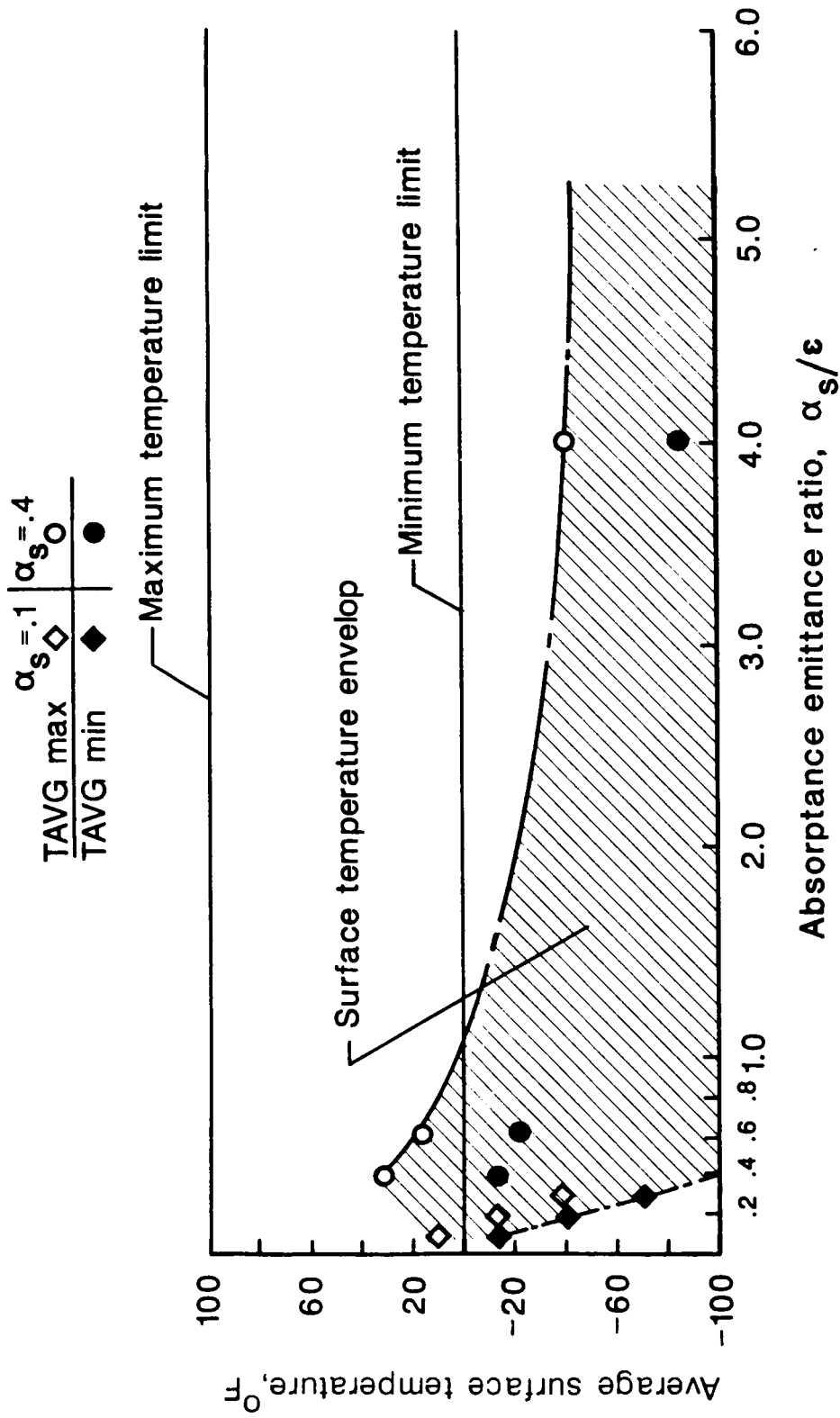


Figure 20. - Average surface temperature envelop for "bottom" radiometer container; $\alpha_s = 0.1$ and 0.4 .

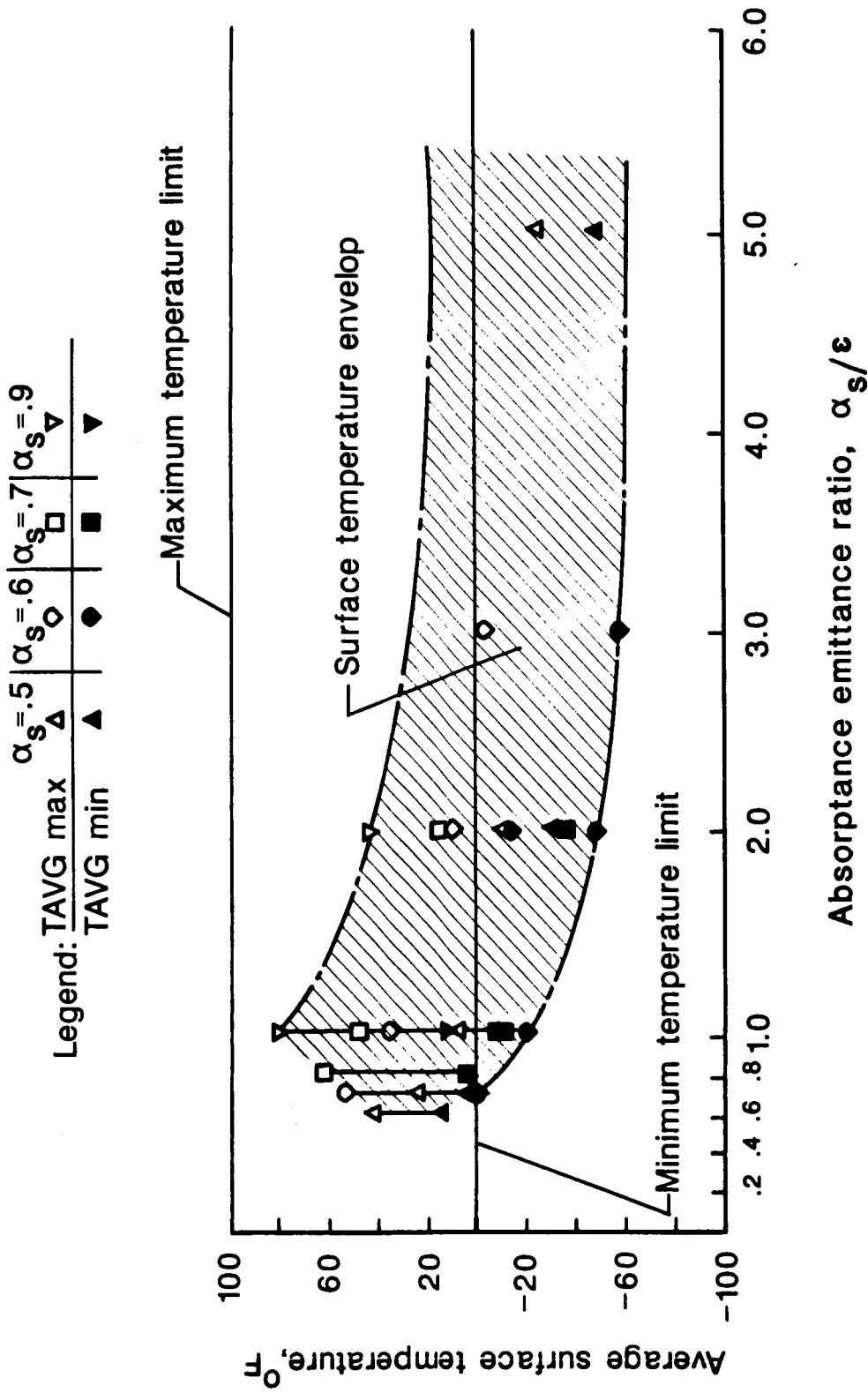
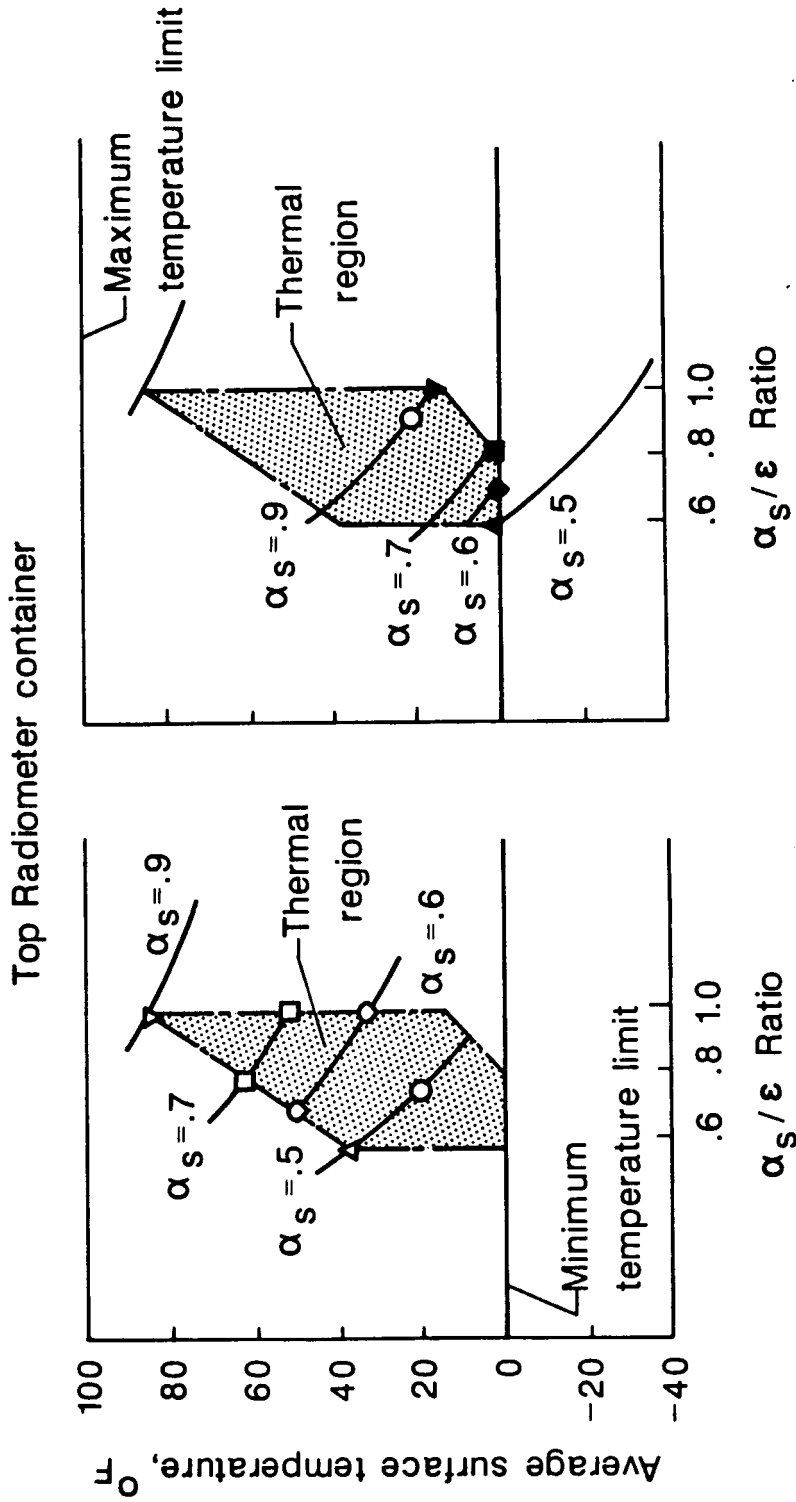


Figure 21. Average surface temperature envelop for "bottom" left radiometer container: $\alpha_s = 0.5, 0.6, 0.7, \text{ and } 0.9$



A. Maximum surface temperature B. Minimum surface temperature

Figure 22. Absorptance selections for maximum or minimum surface temperature

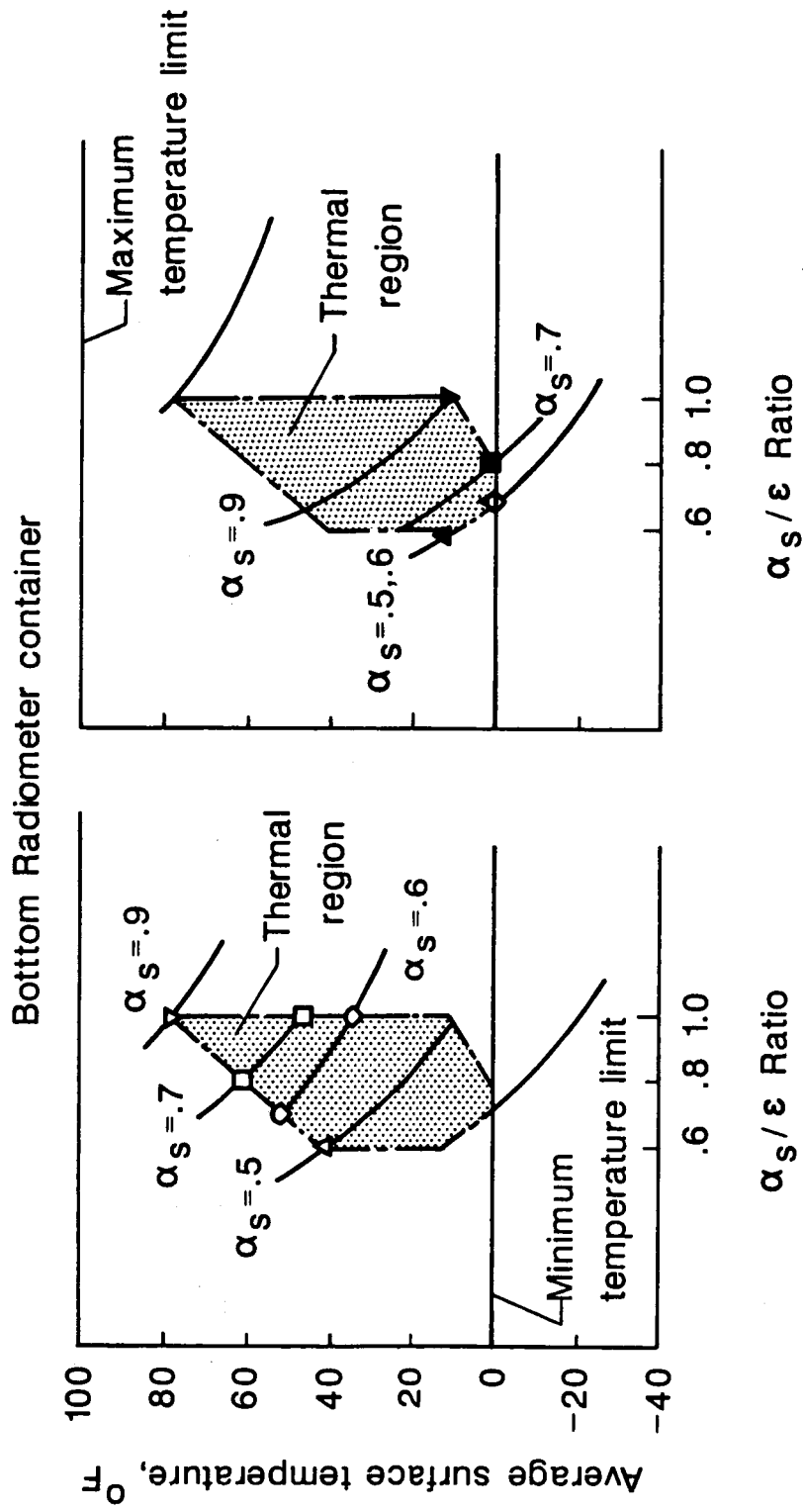


Figure 23. Absorptance selections for maximum or minimum surface temperature

APPENDIX A
TRASYS RADIATION MODEL
AND
MITAS THERMAL MODEL

This appendix contains the two thermal source programs used by TRASYS and MITAS II to calculate heat fluxes and surface temperatures, respectively.

The source program used for TRASYS represents the geometric configuration of the radiometer containers in a 666 km Earth orbit. Inputs required for this program included geometric coordinates, surface properties--absorptance, emittance, and orientation of surfaces with respect to the sun and Earth. The following are partial statements used in the program:

```

SURFN = 1 } node number
TYPE = RECTANGLE } surface shape
PROP =  $\alpha, \epsilon$  } surface properties
P1 = X1, Y1, Z1
P2 = X2, Y2, Z2      geometric coordinates
P3 = X3, Y3, Z3

CALL ORBIT2 (. . . Earth, . . .  $\beta = 90^\circ$ , . . . 666 km) } orbit definition

```

Further details and information about the TRASYS program can be obtained from reference 10 and the Langley Research Center custodian of TRASYS.

The MITAS II source program represents the nodes (capacitance) and conductors (linear and nonlinear) for the surfaces of the three radiometer containers. Inputs include initial temperatures of surfaces, constants for repetitive calculations, relaxation criteria, arrays for the variable heat fluxes of orbit for each surface, orbit time array, and variable absorptance and emittance locations.

Nodal values for each surface were calculated using the relationship:

$$\text{NODE VALUE} = (\text{density}) * (\text{volume}) * (\text{specific heat})$$

Conductor values for each node were calculated using the relationship:

$$\text{Conductor value} = \frac{(\text{area}) * (\text{conductivity})}{\text{length}}$$

Comments in the source program indicate the sun and Earth facing surfaces. Representative statements for nodes and conductors, respectively.

Node	Initial Temperature	Node Value
1,	75,	283.33
Conductor	Start, End	Conductor Value
12,	1,2,	.42

Further information can be found in reference 11 and the Langley Research Center MITAS custodian.

TRASY S SOURCE CODE

HEADER OPTIONS DATA

TITLE 122M HOOP COLUMN TRIPLET FEED

MODEL=FEED3

C **** THESE NEXT TWO CARDS ARE FIRST RUN RESTART CARDS ****

C RSO=RSO1

C RTO=RTO1

C ***** THESE NEXT FOUR CARDS ARE SECOND RUN RESTART FILE NAMES ****

C RSO=RSO2

C RTO=RTO2

C RSI=RSO1

C RTI=RTO1

HEADER SURFACE DATA

D 3.280#CONVERTS METRIC INPUT DIMENSIONS TO FEET

C ***** SUN FACING SURFACE OF TOP FEED (RF TRANSPARENT-KAPTON,F/G,PAINT)

C**** THE EMISSIVITY OF SURFACES 1,2,4,5,6,12,20,21,30,31,32,

C**** 212,220,221,230,231,& 232 IS REDUCED FROM: .7 TO: .5

BCS TOP

S SURFN=1

TYPE=RECT

ACTIVE=BOTTOM

PROP=0.5,0.5

P1=115.922,127.859,7.766

P2=114.522,125.169,7.766

P3=114.522,125.169,-7.766

C ***** RIGHT EDGE (IN RIGHT VIEW) POSSIBLE RADIATOR

S SURFN=2

TYPE=RECT

ACTIVE=BOTTOM

PROP=0.5,0.5

P1=115.922,127.859,-7.766

P2=114.522,125.169,-7.766

P3=114.701,125.074,-7.766

C ***** EARTH FACING SURFACE (POSSIBLY ALUMINUM)

S SURFN=3

TYPE=RECT

ACTIVE=TOP

PROP=0.9,0.9

P1=116.101,127.764,7.766

P2=114.701,125.074,7.766

P3=114.701,125.074,-7.766

C ***** LEFT EDGE (IN RIGHT VIEW) POSSIBLE RADIATOR

S SURFN=4

TYPE=RECT

ACTIVE=TOP

PROP=0.5,0.5

P1=115.922,127.859,7.766

P2=114.522,125.169,7.766

P3=114.701,125.074,7.766

C ***** TOP SURFACE OF TOP FEED
S SURFN=5
TYPE=RECT
ACTIVE=BOTTOM
PROP=0.5,0.5
P1=116.101,127.764,7.766
P2=115.922,127.859,7.766
P3=115.922,127.859,-7.766
C ***** BOTTOM SURFACE OF TOP FEED
S SURFN=6
TYPE=RECT
ACTIVE=TOP
PROP=0.5,0.5
P1=114.701,125.074,7.766
P2=114.522,125.169,7.766
P3=114.522,125.169,-7.766
C F4=117.498,120.490,.8685
C ***** LEFT FEED, SUN FACING SURFACE
BCS LEFT
S SURFN=12
TYPE=POLY
ACTIVE=BOTTOM
PROP=0.5,0.5
P1=115.919,115.368,14.531
P2=117.079,112.662,13.806
P3=117.078,116.204,.5868
P4=116.306,118.130,.6135
P5=115.919,119.031,.8548
C ***** LEFT FEED, RIGHT LOWER, SURFACE
S SURFN=20
TYPE=RECT
ACTIVE=BOTTOM
PROP=0.5,0.5
P1=116.306,118.130,.6135
P2=117.078,116.204,.5868
P3=117.266,116.278,.6066
C ***** LEFT FEED, RIGHT UPPER, SURFACE
S SURFN=21
TYPE=RECT
ACTIVE=BOTTOM
PROP=0.5,0.5
P1=115.918,119.031,.8548
P2=116.306,118.130,.6135
P3=116.492,118.204,.6332
C ***** LEFT FEED, EARTH FACING SURFACE
S SURFN=22
TYPE=POLY
ACTIVE=TOP
PROP=0.9,0.9
P1=116.105,115.442,14.550
P2=117.267,112.737,13.826
P3=117.266,116.278,.6066
P4=116.492,118.204,.6332
P5=116.105,119.106,.8748

ORIGINAL PAGE IS
OF POOR QUALITY

```
C **** LEFT FEED, LEFT SURFACE
S
  SURFN=30
  TYPE=RECT
  ACTIVE=TOP
  PROP=0.5,0.5
  P1=115.919,115.368,14.531
  P2=117.079,112.662,13.806
  P3=117.267,112.737,13.826
C **** LEFT FEED, BOTTOM SURFACE
S
  SURFN=31
  TYPE=RECT
  ACTIVE=TOP
  PROP=0.5,0.5
  P1=117.267,112.737,13.826
  P2=117.079,112.662,13.806
  P3=117.078,116.204,.5868
C **** LEFT FEED, TOP SURFACE
S
  SURFN=32
  TYPE=RECT
  ACTIVE=BOTTOM
  PROP=0.5,0.5
  P1=116.105,115.442,14.550
  P2=115.919,115.368,14.531
  P3=115.918,119.031,.8548
C **** RIGHT FEED, SUN FACING SIDE, IMAGED FROM LEFT FEED
BCS RIGHT, IMGBCS=LEFT, NINC=200, IREF=999, IGEN=ALL
R REFNO=999
  P1=116.838,119.601,0.00
  P2=117.838,119.601,0.00
  P3=117.868,118.601,0.00
HEADER BCS DATA
BCS TOP,0.,0.,0.,0.,0.,0.
BCS LEFT,0.,0.,0.,0.,0.,0.
BCS RIGHT,0.,0.,0.,0.,0.,0.
HEADER OPERATIONS DATA
BUILD FEED3, TOP, LEFT, RIGHT
  CALL NDATA(0,3HALL,0,2HND,0)
C NPLOT$THIS IS NOW A COMMENT CARD ! (NODE PLOTS)
  CALL ORIENT(4HPLAN,1,2,3,0.0,0.0,0.0)
  CALL ORBIT2(3HEAR,0.0,90.0,0.0,0.0,0.0,6.66E5*3.28,0.0)
L FFCAL
C SFCAL
  CALL GBDATA(4HBOTH,0,2HFF)
L GBCAL
  CALL RKDATA(0,2HND,0,100,5HSPACE,99999,0,0,0,0)
L RKCAL
C OPLOT$THIS IS NOW A COMMENT CARD! (ORBIT PLOTS)
  CALL DIDT1(4HNOSH,0,0,0,0,0,2HND,2HND)
ORBGEN CIRP,0.,360.,8,DI
  CALL PLDATA(5HIFALL,3HALL,3HALL,2HND,0,0,0,0,0,0,2HND)
L PLOT
C
END OF DATA
END OF FILE
```

MITAS SOURCE CODE

NOT RESTART
--EOR--

BCD 3TITLE DATA
BCD 9122M HOOP COLUMN TRIPLET FEED STUDY
BCD 9L.A. DILLON-TOMNES 4/84
END

C THIS STUDY IS CONCERNED WITH THREE FEEDS (.3 X 3.5 X 15.5 METER)
C THE UNITS OF THE MODEL PARAMETERS ARE: LENGTH- FEET, TIME- MINUTES
C CONDUCTIVITY- BTU/MIN-F, TEMPERATURE- F, CAPACITANCE- BTU/F.
C *****
C ***** CONDITION: SUN ANGLE= 90 DEGREES *****
C ***** ALTITUDE= 2.1866 FEET (666 KM), *****
C ***** EARTH ORIENTED *****
C ***** IN THIS RUN THE A/E RATIO HAS BEEN CHANGED TO 2.0 ***
C *** THE ABSORPTIVITY HAS BEEN CHANGED TO .9 **
C *** THE EMISSIVITY HAS BEEN CHANGED TO .5, I.E.
C *** TO JUSTIFY THE USAGE OF ALPHA=.5 *****
C *** THIS CHANGE IS MADE IN THE CONSTANTS DATA BLOCK #8 AND #7*****
C----- NODE DATA -----
BCD 3NODE DATA

C----- (BTU/F) -----
1,75.0,128.33*TOP FEED SUN PANEL
2,75.0,3.73*SHORT EDGE RIGHT SIDE
3,75.0,394.9*EARTH PANEL(AL)
4,75.0,3.73*SHORT EDGE LEFT SIDE
5,75.0,18.93*TOP SURFACE
6,75.0,18.93*BOTTOM SURFACE
12,75.0,124.8*LEFT FEED SUN PANEL
13,75.0,87.6*LEFT FEED SUN PANEL
14,75.0,43.0*LEFT FEED SUN PANEL
20,75.0,2.53*LOWER RIGHT SIDE
21,75.0,1.22*UPPER RIGHT SIDE
22,75.0,174.4*EARTH PANEL(AL)
23,75.0,122.6*EARTH PANEL(AL)
24,75.0,60.0*EARTH PANEL(AL)
30,75.0,3.73*LEFT SIDE
31,75.0,16.77*BOTTOM SURFACE
32,75.0,17.0*TOP SURFACE
C ===== DUPLICATION OF LEFT PANEL NODES =====
212,75.0,128.8*RIGHT FEED SUN PANEL
213,75.0,87.6*RIGHT FEED SUN PANEL
214,75.0,43.0*RIGHT FEED SUN PANEL
220,75.0,2.53*LOWER RIGHT SIDE
221,75.0,1.22*UPPER RIGHT SIDE
222,75.0,174.4*EARTH PANEL(AL)
223,75.0,122.6*EARTH PANEL(AL)
224,75.0,60.0*EARTH PANEL(AL)
230,75.0,3.73*RIGHT SIDE
231,75.0,16.77*BOTTOM SURFACE
232,75.0,17.0*TOP SURFACE
-99,-460.0,0.0*DEEP SPACE BOUNDARY NODE
END)

C----- CONDUCTOR DATA -----
BCD 3CONDUCTOR DATA

C----- (BTU/HR-F) -----
12,1,2,.42*TOP FEED SUN PANEL TO RIGHT EDGE
14,1,4,.42* " " LEFT EDGE
15,1,5,7.68*SUN PANEL TO TOP SURFACE
16,1,6,7.68* " " BOTTOM SURFACE
52,5,2,122.4*TOP SURFACE TO RIGHT EDGE
54,5,4,122.4*TOP SURFACE TO LEFT EDGE
62,6,2,122.4* BOTTOM SURFACE TO RIGHT EDGE
64,6,4,122.4* " " LEFT EDGE
32,3,12,.9*EARTH PANEL TO RIGHT EDGE
34,3,4,.9* " " LEFT EDGE
35,3,5,15.42*EARTH SURFACE TO TOP SURFACE
36,3,6,15.42* " " BOTTOM SURFACE
1230,17,13,17.22*LEFT FEED SUN PANEL TO LEFT SIDE
1213,12,13,17.22*SUN PANEL TO SUN PANEL(NODE 12&13)
1214,12,14,15.72* " " " " 12&14
1421,14,21,30*SUN PANEL TO UPPER RIGHT SIDE
1320,13,20,60*SUN PANEL TO LOWER RIGHT SIDE
1432,14,32,17.88*SUN PANEL TO TOP SURFACE
1331,13,31,22.32*SUN PANEL TO BOTTOM SURFACE
2021,20,21,162*LOWER RIGHT SIDE TO LOWER RIGHT SIDE
2132,21,32,162*UPPER RIGHT SIDE TO UPPER RIGHT SIDE
3230,32,30,162*TOP SURFACE TO TOP SURFACE
3031,30,31,168*EARTH PANEL TO LEFT SIDE
2230,22,30,1.68*EARTH PANEL TO RIGHT SIDE
2223,22,23,37.98*EARTH PANEL TO EARTH PANEL(NODE 22&23)
2224,22,24,34.62* " " " " 22&24
2421,24,21,66*EARTH PANEL TO UPPER RIGHT SIDE
2320,23,20,1.26* " " " " LOWER " "
2432,24,32,31.56*EARTH PANEL TO TOP SURFACE
2331,23,31,37.38*EARTH PANEL TO BOTTOM SURFACE
21230,212,230,84*RIGHT FEED SUN PANEL TO RIGHT SIDE
212213,212,213,17.22*SUN PANEL TO SUN PANEL(NODE 212&213)
212214,212,214,15.72* " " " " 212&214
214221,214,221,30*SUN PANEL TO UPPER RIGHT SIDE
213220,213,220,60*SUN PANEL TO LOWER RIGHT SIDE
21432,214,232,17.88*SUN PANEL TO TOP SURFACE
21331,213,231,22.32*SUN PANEL TO BOTTOM SURFACE
220221,220,221,162*BOTTOM SURFACE TO LOWER RIGHT SIDE
221232,221,232,162*LOWER RIGHT SIDE TO UPPER RIGHT SIDE
221232,221,232,162*UPPER RIGHT SIDE TO TOP SURFACE
232230,232,230,168*TOP SURFACE TO LEFT SIDE
230231,230,231,168*LEFT SIDE TO BOTTOM SURFACE
222230,222,230,1.68*EARTH PANEL TO LEFT SIDE
222223,222,223,37.98*EARTH PANEL TO EARTH PANEL(NODE 22&23)
222224,222,224,34.62* " " " " 22&24
224221,224,221,66*EARTH PANEL TO UPPER RIGHT SIDE
223220,223,220,1.26* " " " " LOWER " "

```

22432,224,232,31.56$EARTH PANEL TO TOP SURFACE
22331,223,231,37.38$EARTH PANEL TO BOTTOM SURFACE
C----- RADIATION TO DEEP SPACE CONDUCTORS -----
C**** THE RAD CONDUCTORS REPRESENTS "FA", DOES NOT INCLUDE "STEPHEN-
C***** BOLTZMAN'S CONSTANT" OR "EMISSIVITY". *****
-199,1,99,4560E3; TOP FEED(TF) SUN PANEL TO SPACE
-299,2,99,5930E1$TF; RIGHT SIDE
-399,3,99,4479E3$ TF; EARTH PANEL
-499,4,99,5930E1$TF; LEFT SIDE
-599,5,99,3048E2$TF; TOP SURFACE
-699,6,99,2990E2$TF; BOTTOM SURFACE
-1299,12,99,2008E3$LEFT FEED(LF) SUN PANEL TO SPACE
-1399,13,99,1406E3$
-1499,14,99,6914E2$
-21299,212,99,2008E3$
-21399,213,99,1406E3$
-21499,214,99,6914E2$
-2399,23,99,1393E3$
-2499,24,99,6831E2$
-22399,223,99,1393E3$
-22499,224,99,6831E2$
-2299,22,99,2002E3$LF; EARTH PANEL TO SPACE
-2099,20,99,3775E1$LF; LOWER RT SIDE TO SPACE
-2199,21,99,1824E1$LF; UPPER RT SIDE
-3099,30,99,5971E1$LF; LEFT SIDE TO SPACE
-3199,31,99,2695E2$LF; BOTTOM SURFACE TO SPACE
-3299,32,99,2651E2$LF; TOP SURFACE TO SPACE
-22099,220,99,2002E3$LF; EARTH PANEL TO SPACE
-22099,220,99,3775E1$LF; LOWER RT SIDE TO SPACE
-22199,221,99,1824E1$LF; UPPER RT SIDE
-23099,230,99,5971E1$LF; LEFT SIDE TO SPACE
-23199,231,99,2695E2$LF; BOTTOM SURFACE TO SPACE
-23299,232,99,2651E2$LF; TOP SURFACE TO SPACE
-320,3,20,5644E-1$TF; EARTH PANEL TO LF; LOWER RT SIDE
-321,3,21,5624E-1$
-322,3,22,6584E1$
-323,3,23,1447E1$
-324,3,24,9191$
-3223,3,223,1447E1$
-3224,3,224,9191$
-322,3,22,9351$
-422,4,22,1286E-1$TF; LEFT SIDE TO LF; EARTH PANEL
-423,4,23,1940E-2$
-424,4,24,1275E-2$
-4223,4,223,1940E-2$
-4224,4,224,1275E-2$
-432,4,32,4250E-2$
-620,6,20,5779E-3$TF; BOTTOM SURFACE TO LF; LOWER RT SIDE
-621,6,21,6440E-3$
-622,6,22,3397E-3$
-623,6,23,7430E-3$

```

```

-624,6,24,5315E-1$
-623,6,23,7430E-1$
-6224,6,224,5315E-1$
-632,6,32,1143$
-20230,20,220,2012$
-20221,20,221,2945E-1$
-21220,21,220,2945E-1$
-21221,21,221,4333E-1$
END
BCD 3CONSTANTS DATA
TIMED=0.0
TIME=6.232$ THIS TIME REPRESENTS 4 ORBITS(HOURS)
TSTEP=0.0666$ HOURS; EQUIVALENT TO 4 MINUTES
C----- RELAXATION CRITERIA -----
NDSTOR=300
DRLXCA=.001
ARLXCA=.001
ITERMX=100
EXTLIM=30.0
C----- PROBLEM UNITS -----
ABSZRO=-460.0
SBCNST=.1713E-8$ STEFAN-BOLTZMAN CONSTANT (BTU/HR-(FT)**2 - (F)**4)
1=.01400$ ***** THESE CONSTANTS ARE THE PLANETARY DIRECT **
2=17.817$ ** INCIDENT FLUXES FOR EACH NODE DURING **
3=55.542$ ** AN ORBIT. **
4=17.817$ ** THE UNITS ARE: BTU/HR-(FT)**2 **
5=34.884$ ***** ABSORPTIVITY *****
6=5.5490$ ***** EMISSIVITY OR ABSORPTIVITY *****
7=.70$ SOLAR ABSORPTIVITY
8=.50$ ***** THESE CONSTANTS ARE ALSO PLANETARY DIRECT **
12=0.0$ ***** INCIDENT FLUXES FOR *****
14=0.0 ***** THE APPROPRIATE NODES *****
20=20.703$ ** INCIDENT FLUXES FOR *****
21=17.722$ ** THE APPROPRIATE NODES *****
22=57.823$ ***** ABSORPTIVITY *****
23=57.828
24=57.829
30=17.746$ ***** ABSORPTIVITY *****
31=31.316$ ***** EMISSIVITY OR ABSORPTIVITY *****
32=7.950$ ***** INCIDENT FLUXES FOR *****
212=0.0$ ***** THE APPROPRIATE NODES *****
214=0.0$ ***** ABSORPTIVITY *****
220=20.291$ ***** EMISSIVITY OR ABSORPTIVITY *****
221=17.719$ ***** INCIDENT FLUXES FOR *****
222=57.818$ ***** THE APPROPRIATE NODES *****
223=57.828$ ***** ABSORPTIVITY *****
224=57.829$ ***** INCIDENT FLUXES FOR *****
230=17.744$ ***** THE APPROPRIATE NODES *****
231=3.386$ ***** ABSORPTIVITY *****
232=7.808$ ***** EMISSIVITY OR ABSORPTIVITY *****
END

```

ORIGINAL PAGE IS OF POOR QUALITY

```

C      BCD ZARRAY DATA
C*****
C*** THESE ARRAYS ARE OF THE COMBINED SOLAR & ALBEDO *****
C*** DIRECT INCIDENT FLUXES NEEDED TO CALCULATE THE *****
C*** HEAT LOAD FOR EACH NODE; DONE IN THE EXECUTION *****
C*** BLOCK. THOUGHT!; TRAYSIS IS THE PLACE WHERE I *****
C*** MANIPULATE THE ALPHA'S & EMMIS' TO CHANGE *****
C*** SOLAR & ALBEDO DIRECT INCIDENT FLUXES *****
C*****
C      NODE 1 ;BTU/HR-FT**2
C      1, 380.57,409.15,158.06,18.47,SPACE,7
C      129.05,380.57,END
C
C      NODE 2
C      2, 30.08,21.27,1.05,0.0,0.0,0.0,0.0,0.0,0.0,0.0,0.0
C      1.05,21.27,30.08,END
C
C      NODE 3
C      3, 94.39,64.41,1.56,0.0,0.0,0.0,0.0,0.0,0.0,0.0,0.0,202.91
C      69.08,94.39,END
C
C      NODE 4
C      4, 30.08,21.27,1.21,0.0,0.0,0.0,0.0,0.0,0.0,0.0,0.0,1.21
C      21.27,30.08,END
C
C      NODE 5
C      5, 59.15,170.92,383.80,428.44,0.0,0.0,0.0,0.0,0.0,0.0,0.0
C      13.38,48.59,15.15,END
C
C      NODE 6
C      6, 210.41,5.45,0.0,0.0,0.0,0.0,0.0,0.0,0.0,0.0,0.0,258.81
C      380.53,417.86,210.41,END
C
C      NODE 12
C      12, 396.36,168.38,0.0,0.0,0.0,0.0,0.0,0.0,0.0,0.0,0.0,158.32
C      392.28,396.45,END
C
C      NODE 13
C      13, 396.36,168.38,0.0,0.0,0.0,0.0,0.0,0.0,0.0,0.0,0.0,158.32
C      392.28,396.45,END
C
C      NODE 14
C      14, 396.36,168.38,0.0,0.0,0.0,0.0,0.0,0.0,0.0,0.0,0.0,158.32
C      392.28,396.45,END
C
C      NODE 20
C      20, 34.99,24.88,21.80,34.17,0.0,0.0,0.0,0.0,0.0,0.0,0.0,1.12
C      24.60,34.99,END
C
C      NODE 21
C      21, 30.09,100.26,112.30,100.28,0.0,0.0,0.0,0.0,0.0,0.0,0.0
C      60.20,48.30,09,END
C
C      NODE 22
C      22, 98.26,71.35,163.50,311.55,0.0,0.0,0.0,0.0,0.0,0.0,0.0,23.70
C      2.02,67.60,98.26,END
C
C      NODE 23
C      23, 98.26,71.35,163.50,311.55,0.0,0.0,0.0,0.0,0.0,0.0,0.0,23.70
C      2.02,67.60,98.26,END
C
C      NODE 24
C      24, 98.26,71.35,163.50,311.55,0.0,0.0,0.0,0.0,0.0,0.0,0.0,23.70
C      2.02,67.60,98.26,END
C
C      NODE 230
C      230, 29.97,20.56,78.0,0.0,0.0,0.0,0.0,0.0,0.0,0.0,0.0,100.57,112.59
C      100.14,29.97,END
C
C      NODE 231
C      231, 53.07,34.36,66.0,0.0,0.0,0.0,0.0,0.0,0.0,0.0,0.0,416.28
C      387.80,196.37,53.07,END
C
C      NODE 232
C      232, 170.14,394.47,387.73,283.18,0.0,0.0,0.0,0.0,0.0,0.0,0.0,0.0
C      8.03,170.14,END
C
C      NODE 212
C      212, 396.36,168.38,0.0,0.0,0.0,0.0,0.0,0.0,0.0,0.0,0.0,158.32
C      392.28,396.45,END
C
C      NODE 213
C      213, 396.36,168.38,0.0,0.0,0.0,0.0,0.0,0.0,0.0,0.0,0.0,158.32
C      392.28,396.45,END
C
C      NODE 214
C      214, 396.36,168.38,0.0,0.0,0.0,0.0,0.0,0.0,0.0,0.0,0.0,158.32
C      392.28,396.45,END
C
C      NODE 220
C      220, 34.99,24.88,21.80,34.17,0.0,0.0,0.0,0.0,0.0,0.0,0.0,1.12
C      24.60,34.99,END
C
C      NODE 221
C      221, 30.09,100.26,112.30,100.28,0.0,0.0,0.0,0.0,0.0,0.0,0.0
C      60.20,48.30,09,END
C
C      NODE 222
C      222, 98.26,71.35,163.50,311.55,0.0,0.0,0.0,0.0,0.0,0.0,0.0,23.70
C      2.02,67.60,98.26,END
C
C      NODE 223
C      223, 98.26,71.35,163.50,311.55,0.0,0.0,0.0,0.0,0.0,0.0,0.0,23.70
C      2.02,67.60,98.26,END
C
C      NODE 224
C      224, 98.26,71.35,163.50,311.55,0.0,0.0,0.0,0.0,0.0,0.0,0.0,23.70
C      2.02,67.60,98.26,END
C
C      NODE 230
C      230, 29.97,20.56,78.0,0.0,0.0,0.0,0.0,0.0,0.0,0.0,0.0,100.57,112.59
C      100.14,29.97,END
C
C      NODE 231
C      231, 53.07,34.36,66.0,0.0,0.0,0.0,0.0,0.0,0.0,0.0,0.0,416.28
C      387.80,196.37,53.07,END
C
C      NODE 232
C      232, 170.14,394.47,387.73,283.18,0.0,0.0,0.0,0.0,0.0,0.0,0.0,0.0
C      8.03,170.14,END

```

```

C ORBIT TIME ARRAY (HOURS)
  7, 0.00,1.95,1.389,1.480,1.584,1.688,1.779,1.974
  1.077,1.1076,1.1168,1.1363,1.1558,END
C
C RCD SEEXECUTION
DO 50 I=1,13
A1+I=((A1+I)*R7+(R1*R8))*506.73)* ABSORBED HEAT FOR NODE 1
C*****
C**** A1 IS FIRST, THE ARRAY WHICH HAS THE VALUES OF SOLAR ***
C**** PLUS ALBEDO FLUXES. SECOND, THESE VALUES ARE REDEFINED *
C**** IN THE COMPUTER'S MEMORY AS THE VALUES OF TOTAL ***
C**** ABSORBED HEAT FOR THAT NODE WHICH IS CALCULATED ABOVE **
C**** R1 IS THE CONSTANT WHICH DEFINES THE PLANETARY FLUX ***
C**** FOR THAT NODE, R7=SOLAR ABSORPTIVITY,R8=EMISSIVITY ***
C*****
A2+I=((A2+I)*R7+(R2*R8))*6.61)
A3+I=((A3+I)*R8+(R3*R8))*506.73)
A4+I=((A4+I)*R7+(R4*R8))*6.61)
A5+I=((A5+I)*R7+(R5*R8))*33.86)
A6+I=((A6+I)*R7+(R6*R8))*33.86)
A12+I=((A12+I)*R7+(R12*R8))*223.22)
A13+I=((A13+I)*R7+(R13*R8))*156.46)
A14+I=((A14+I)*R7+(R14*R8))*76.91)
A20+I=((A20+I)*R7+(R20*R8))*4.53)
A21+I=((A21+I)*R7+(R21*R8))*2.19)
A22+I=((A22+I)*R8+(R22*R8))*223.19)
A23+I=((A23+I)*R8+(R23*R8))*156.51)
A24+I=((A24+I)*R8+(R24*R8))*76.98)
A30+I=((A30+I)*R7+(R30*R8))*6.63)
A31+I=((A31+I)*R7+(R31*R8))*29.95)
A32+I=((A32+I)*R7+(R32*R8))*30.63)
A212+I=((A212+I)*R7+(R212*R8))*223.22)
A213+I=((A213+I)*R7+(R213*R8))*156.46)
A220+I=((A220+I)*R7+(R220*R8))*4.53)
A221+I=((A221+I)*R7+(R221*R8))*2.19)
A222+I=((A222+I)*R8+(R222*R8))*223.19)
A223+I=((A223+I)*R8+(R223*R8))*156.51)
A224+I=((A224+I)*R8+(R224*R8))*76.98)
A230+I=((A230+I)*R7+(R230*R8))*6.63)
A231+I=((A231+I)*R7+(R231*R8))*29.95)
A232+I=((A232+I)*R7+(R232*R8))*30.63)
F 50 CONTINUE
C
FORWRD
HETRAL
QMAP(1HD)
QMAP(1HD)
ENDFILE NUSER1
ENDFILE NUSER2
END
C

```

ORIGINAL PAGE IS OF POOR QUALITY

```

C BCD SVARIABLES 1
C***** CYCLIC INTERPOLATION OF THE PREVIOUSLY *****
C***** CALCULATED HEAT LOADS FOR EACH NODE AND *****
C***** TIME IN ORBIT WILL BE DONE HERE. *****
C*****
C ARRAY A7=ORBIT INCREMENTAL TIME FOR ONE PERIOD (HOURS)
C ARRAY A1,A2,ETC.=CALCULATED HEAT LOADS FOR EACH NODE (RTU/HR)
C Q1,Q2,ETC.=HEAT INPUT TO NODE FOR EACH INCREMENT OF TIME
C WITHIN A PERIOD.
C
DA11CY(1.558,TIME,A7,A1,Q1)
DA11CY(1.558,TIME,A7,A2,Q2)
DA11CY(1.558,TIME,A7,A3,Q3)
DA11CY(1.558,TIME,A7,A4,Q4)
DA11CY(1.558,TIME,A7,A5,Q5)
DA11CY(1.558,TIME,A7,A6,Q6)
DA11CY(1.558,TIME,A7,A12,Q12)
DA11CY(1.558,TIME,A7,A13,Q13)
DA11CY(1.558,TIME,A7,A14,Q14)
DA11CY(1.558,TIME,A7,A20,Q20)
DA11CY(1.558,TIME,A7,A21,Q21)
DA11CY(1.558,TIME,A7,A22,Q22)
DA11CY(1.558,TIME,A7,A23,Q23)
DA11CY(1.558,TIME,A7,A24,Q24)
DA11CY(1.558,TIME,A7,A30,Q30)
DA11CY(1.558,TIME,A7,A31,Q31)
DA11CY(1.558,TIME,A7,A32,Q32)
DA11CY(1.558,TIME,A7,A212,Q212)
DA11CY(1.558,TIME,A7,A213,Q213)
DA11CY(1.558,TIME,A7,A214,Q214)
DA11CY(1.558,TIME,A7,A221,Q221)
DA11CY(1.558,TIME,A7,A222,Q222)
DA11CY(1.558,TIME,A7,A223,Q223)
DA11CY(1.558,TIME,A7,A224,Q224)
DA11CY(1.558,TIME,A7,A230,Q230)
DA11CY(1.558,TIME,A7,A231,Q231)
DA11CY(1.558,TIME,A7,A232,Q232)
END
C***** SAVE TEMPERATURES *****
C BCD SOUTPUT CALLS
OTIME=TIME
TFRINT
WRITE (NUSER1,20)OTIM,T1,T2,T3,T4,T5,T6,T12,T13,T14
F 20 FORMAT(10(3X,F7.3))
C***** OTIME=TIME (MINUTES),T1=TF;SUN PANEL,T2=TF;RIGHT SIDE
C***** T3=TF;EARTH PANEL,T4=TF;LEFT SIDE,T5=TF;TOP SURFACE
C***** T6=TF;BOTTOM SURFACE,T12&T13&T14=LF;SUN PANEL
C***** T20=LF;RT LOWER SIDE,T21=LF;RT UPPER SIDE
C***** T22,T23,T24=LF;EARTH PANEL,T30=LF;LEFT SIDE
C***** T31=LF;BOTTOM SURFACE,T32=LF;TOP SURFACE
C*****
WRITE (NUSER2,21)OTIM,T20,T21,T22,T23,T24,T30,T31,T32
F 21 FORMAT(9(3X,F7.3))
C
C BCD SEND OF DATA
C THE DRIVER FILE=CAR; FIRST TEMPERATURE FILE=CAN1
C SECOND TEMPERATURE FILE = CAN2
C
WRITE (NUSER1,20)OTIM,T1,T2,T3,T4,T5,T6,T12,T13,T14
END
C THE DRIVER FILE=CAR; FIRST TEMPERATURE FILE=CAN1
END OF FILE

```

"AVERAGE" SURFACE TEMPERATURE
APPENDIX B

This appendix presents the temperatures for the top and bottom radiometer containers for the absorptance and emittance values studied. Each surface was examined for its maximum and minimum temperatures for each orbit. Maximum and minimum temperatures for all surfaces were selected at the following orbit times:

<u>Orbit</u>	<u>TAVGMAX</u>	<u>TAVGMIN</u>
2	1.6 hrs.	2.8 hrs.
3	3.6 hrs.	4.3 hrs.
4	5.2 hrs.	5.9 hrs.

Orbit 1 was not used because the containers had not been exposed to a complete thermal cycle--full sun-to-full shadow exposure.

The calculated "average" surface temperatures for the top and bottom containers were determined by using equation 1.

Top Radiometer Container

α_s	ϵ	α_s/ϵ	TAVGMAX, ($^{\circ}$ F)	TAVGMIN, ($^{\circ}$ F)
.1	.9	.1	-21	-38
.1	.6	.2	-45	-63
.1	.3	.3	-77	-96
.4	.9	.4	24	-16
.4	.7	.6	12	-28
.4	.1	4.0	-48	-80
.5	.9	.6	38	2
.5	.7	.7	24	-14
.5	.5	1.0	5	-13
.5	.3	2.0	-18	-52
.5	.1	5.0	-40	-77
.6	.9	.7	50	0
.6	.6	1.0	32	-18
.6	.3	2.0	6	-45
.6	.2	3.0	-4	-53
.7	.9	.8	62	2
.7	.7	1.0	52	-7
.7	.3	2.0	21	-40
.9	.9	1.0	82	14
.9	.5	2.0	61	-10

Table B1.- Calculated "average" surface temperatures for the "top" radiometer container

Bottom Radiometer Container

α_s	ϵ	α_s / ϵ	TAVGMAX, ($^{\circ}$ F)	TAVGMIN, ($^{\circ}$ F)
.1	.9	.1	-16	8
.1	.6	.2	-42	-15
.1	.3	.3	-72	-40
.4	.9	.4	30	-15
.4	.7	.6	14	-24
.4	.1	4.0	-42	-86
.5	.9	.6	41	13
.5	.7	.7	23	1
.5	.5	1.0	6	-13
.5	.3	2.0	-12	-31
.5	.1	5.0	-26	-50
.6	.9	.7	51	-3
.6	.6	1.0	34	-22
.6	.3	2.0	7	-50
.6	.2	3.0	-5	-59
.7	.9	.8	60	2
.7	.7	1.0	46	-11
.7	.3	2.0	14	-43
.9	.9	1.0	79	9
.9	.5	2.0	42	-17

Table B2.- Calculated "average" surface temperatures
for the "bottom" radiometer container.

Standard Bibliographic Page

1. Report No. NASA TM-89026	2. Government Accession No.	3. Recipient's Catalog No.	
4. Title and Subtitle Thermal Analysis of Radiometer Containers for the 122m Hoop Column Antenna Concept		5. Report Date September 1986	6. Performing Organization Code 506-43-51-04
		8. Performing Organization Report No.	
7. Author(s) Lawrence A. Dillon-Townes		10. Work Unit No.	
9. Performing Organization Name and Address NASA Langley Research Center Hampton, VA 23665-5225		11. Contract or Grant No.	
		13. Type of Report and Period Covered Technical Memorandum	
12. Sponsoring Agency Name and Address National Aeronautics and Space Administration Washington, DC 20546		14. Sponsoring Agency Code	
		15. Supplementary Notes	
16. Abstract A thermal analysis has been conducted for the 122 Meter Hoop Column Antenna (HCA) Radiometer electronic package containers. The HCA radiometer containers were modeled using the computer aided graphics program--ANVIL 4000, and thermally simulated using two thermal programs--TRASYS and MITAS. The results of the analysis provided relationships between the absorptance-emittance ratio (α_s/ϵ) and the "average" surface temperature of the orbiting radiometer containers. These relationships can be used to specify the surface properties--absorptance and reflectance, of the radiometer containers. This study is an initial effort in determining the passive thermal protection needs for the 122 m HCA radiometer containers. Several recommendations are provided which expand this effort so specific passive and active thermal protection systems can be defined and designed.			
17. Key Words (Suggested by Authors(s)) 122m Hoop Column Antenna Radiometer Thermal Analyzer (MITAS) Radiation Analyzer (TRASYS) Orbital Analysis		18. Distribution Statement Unclassified - Unlimited Subject Category 34	
19. Security Classif.(of this report) Unclassified	20. Security Classif.(of this page) Unclassified	21. No. of Pages 52	22. Price A04